AGU PUBLICATIONS

Tectonics

RESEARCH ARTICLE
10.1002/2016TC004198

Key Points:
- Interpretation of new multichannel seismic profiles acquired in the eastern margin of the Tyrrhenian Sea
- Reconstruction of the geometric and kinematics aspects of a segmented back-arc margin
- Interaction between extensional and transtensional tectonics along an oblique back-arc basin setting

Correspondence to:
A. Conti,
alessia.conti@uniroma1.it

Citation:
Conti, A., S. Bigi, M. Cuffaro, C. Doglioni, D. Scrocca, F. Muccini, L. Cocchi, M. Ligi, and G. Bortoluzzi (2017), Transfer zones in an oblique back-arc basin setting: Insights from the Latium-Campania segmented margin (Tyrrhenian Sea), *Tectonics*, *36*, 78–107, doi:10.1002/2016TC004198.

Received 29 MAR 2016
Accepted 14 DEC 2016
Accepted article online 16 DEC 2016
Published online 20 JAN 2017

Transfer zones in an oblique back-arc basin setting: Insights from the Latium-Campania segmented margin (Tyrrhenian Sea)

A. Conti[1], S. Bigi[1], M. Cuffaro[2], C. Doglioni[1,3], D. Scrocca[2], F. Muccini[3], L. Cocchi[3], M. Ligi[4], and G. Bortoluzzi[4]

[1]Dipartimento di Scienze della Terra, Università Sapienza, Rome, Italy, [2]Istituto di Geologia Ambientale e Geoingegneria, CNR, Rome, Italy, [3]Istituto Nazionale di Geofisica e Vulcanologia, Rome, Italy, [4]Istituto di Scienze Marine, CNR, Bologna, Italy

Abstract New multichannel seismic reflection profiles were acquired to unravel the structure of a portion of the eastern margin of the Tyrrhenian basin. This extensional feature is part of an Oligocene to Present back-arc basin in the hangingwall of the west directed Apennines subduction system. The basin provides excellent conditions to investigate the early stage processes leading to the development of rifted passive margins and to the emplacement of oceanic crust in an oblique setting. The interpreted post-stack-migrated seismic profiles highlight the geometry and kinematics of the Pontine escarpment that connects the Latium-Campania continental margin to the Vavilov basin. The latter is the main feature of the area, related to the early Pliocene extension of the Tyrrhenian Sea. Several morphological variations are pointed out along strike, mirroring different structural settings of the margin itself: a steeper margin to the north corresponds to high-angle possibly transtensional faults, whereas a smooth slope in the southern portion corresponds to several more distributed listric faults. This work contributes to the understanding of the interplay between extensional and transtensional tectonics along the margins of an oblique back-arc basin.

1. Introduction

The extensional forces acting on the continental lithosphere may lead to the formation of rifted basins that may or may not evolve into a full continental breakup and oceanization, forming two conjugate passive continental margins on each side of the rift.

Back-arc basins are a particular case of extensional basins related to the geodynamic setting of convergent margins, where extension is strictly connected to the rate and the direction of subduction [*Doglioni et al.*, 1999; *Greve et al.*, 2014; *Marcuson et al.*, 2014, among many others]. Generally, slab rollback is considered the main driving mechanism, which determines the extension of the overriding plate and the formation of extensional basins when the subduction hinge migrates away relative to the upper plate [*Doglioni et al.*, 2007].

Several back-arc basins characterize the western Mediterranean region, associated with the west directed subduction of the Adria plate under the European plate, active since late Eocene-Oligocene [*Carminati et al.*, 2012]. Extension started in the central-northern part of the western Mediterranean Sea with the eastward propagation of the opening of several triangular subbasins, separated by slices of boudinaged continental lithosphere [*Gueguen et al.*, 1997]. The subbasins are the Ligurian-Provencal basin (~30–20 Ma) and its southwestern prolongation into the Valencia Trough (~30–20 Ma), the Alborán basin (~20–0 Ma) to the west, and the Algerian basin (~25–20 Ma) southward [*Lustrino et al.*, 2011, and references therein]. The Tyrrhenian Sea is the youngest of these basins, and its opening is linked to the eastward migration of the Apennines-Calabrian subduction system, from Tortonian to Present (Figure 1). Several geological and geophysical studies have been carried out in this area, highlighting a complex crustal structure of the basin; the Italian and Sardinia margins are usually interpreted as stretched continental crust, whereas several studies suggest the presence of oceanic crust in the central abyssal plains, the Vavilov and Marsili basins [*Mascle and Rehault*, 1990; *Sartori et al.*, 2004; *Cella et al.*, 2008; *Scrocca et al.*, 2012] (Figure 1).

The kinematic of back-arc basins is controlled by either proximal or far field stresses [*Martinez et al.*, 2007], so that subduction system changes result in variations on the mode of basin opening. This can be observed, for example, in the geometries of the western Mediterranean basins, which are the result of changes in the subduction system configuration [*Jolivet et al.*, 2008; *Schettino and Turco*, 2011].

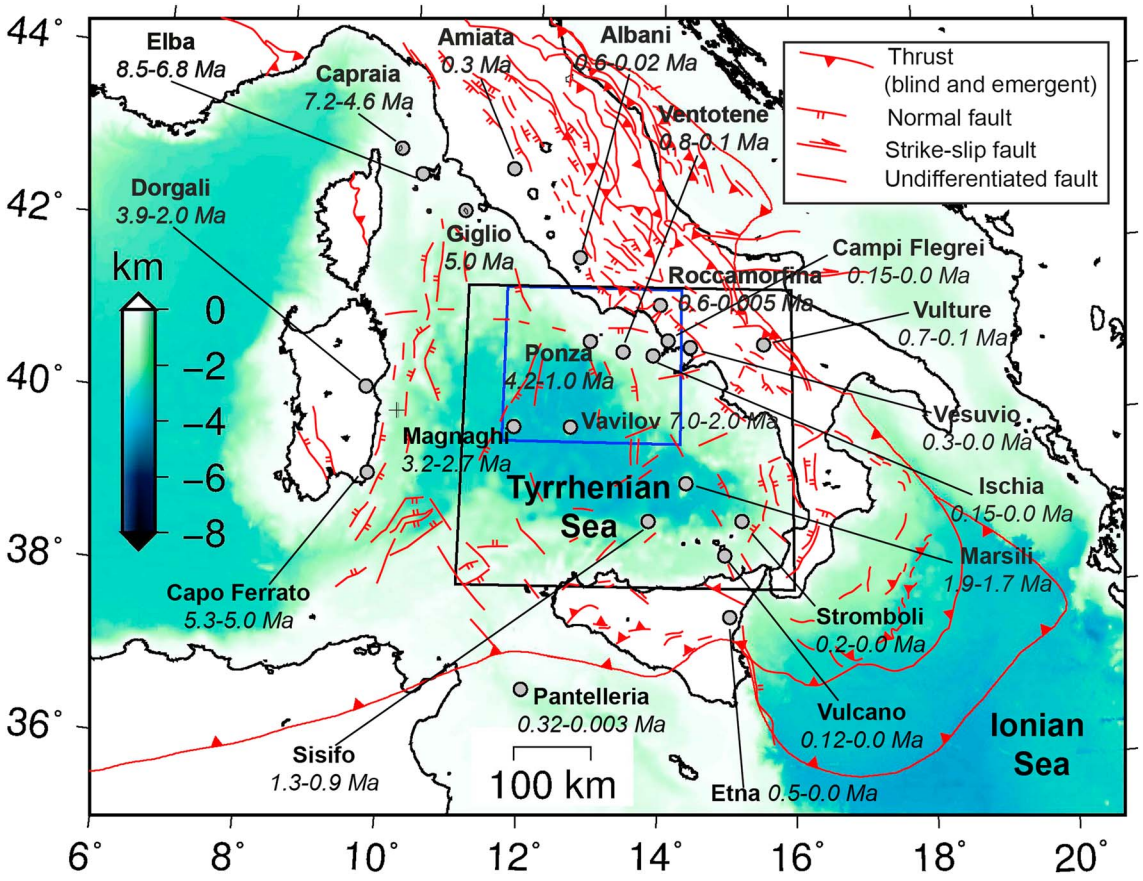

Figure 1. Synthetic tectonic map of Italy showing main structural features associated to the Apennines-Calabrian subduction system and to the back-arc domain. In the Vavilov and Marsili basins the presence of oceanic crust is inferred. Dots represent the distribution of Cenozoic igneous products in the Tyrrhenian and circum-Tyrrhenian region; a general east and southeastward migration in both space and time is observed. The black and blue boxes represent location of Figures 2 and 3, respectively. Figure modified after *Scrocca et al.* [2003a, 2003b] and *Carminati and Doglioni* [2012].

We present here 2-D seismic reflection data obtained during cruise TIR-10 with the R/V *Urania* from an area of the Latium-Campania margin of the Tyrrhenian Sea, in particular from offshore Anzio to Gaeta, within the Pontine islands area (Figure 1). In this area, a steep escarpment connects the Italian continental margin to the Vavilov basin; it is one of the most relevant geomorphological features of the whole Mediterranean, deepening from −200 m to −3000 m in less than 15 km. In spite of its relevant regional morphology, the geometry and kinematics of this area are still poorly constrained. In addition, the study area is located at the transition between the Northern Tyrrhenian domain and the Southern Tyrrhenian domain, conventionally located along the 41° Parallel Line, a regional magnetic and free-air gravity anomaly whose structural significance is still debated [*Malinverno and Ryan*, 1986; *Kastens and Mascle*, 1990; *Doglioni*, 1991; *Spadini and Wezel*, 1994; *Carminati et al.*, 1998; *Bruno et al.*, 2000; *Faccena et al.*, 2001] (Figure 1). The northern Tyrrhenian domain is characterized by a maximum depth of 2000–2200 m, 20 km thick continental crust, low heat flow values (from 80 to 120 m Wm^{-2} [*Della Vedova et al.*, 1984]) and positive Bouguer anomaly (from 80 to 120 mGal [*Caratori Tontini et al.*, 2007]). The seafloor morphology is characterized by N-S trending ridges. The southern domain is deeper, reaching 3600 m, and has a thinner crust, about 10 km thick, with deep basins (Vavilov and Marsili basins) characterized by Pliocene to recent mid-ocean ridge basalt (MORB)-type basalts [*Kastens et al.*, 1988]. High heat flow values (>250 m Wm^{-2}) measured in the Marsili basin [*Della Vedova et al.*, 1984; *Zito et al.*, 2003] provide evidence of lithospheric stretching in the back-arc basin. Gravity data inversion provides information about apparent density distribution of Marsili-Vavilov basin [*Caratori Tontini et al.*, 2008], suggesting the presence of high-density rocks (density rocks 2900 kg/m^3) which well constrains the hypothesis of a seafloor basin carpeted by oceanic crust.

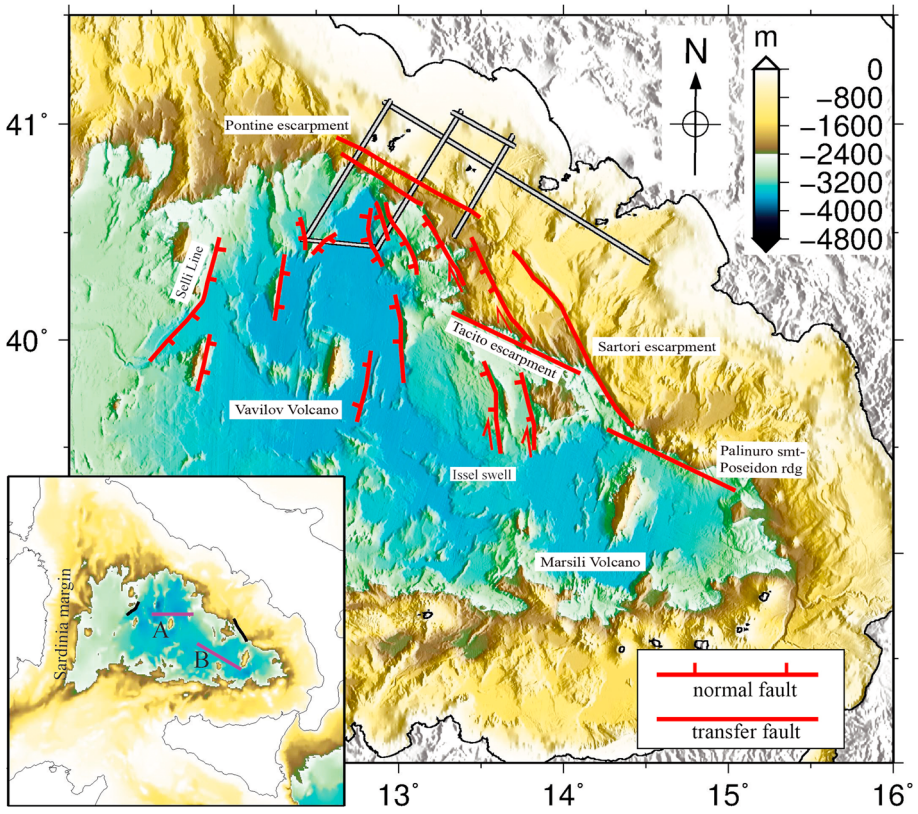

Figure 2. Bathymetric map showing conjugate margins of the Tyrrhenian Sea (smaller box to the left) and the main tectonic lineaments along the central-eastern Tyrrhenian margin and in the Vavilov basin. The two main volcanic edifices, the Vavilov and the Marsili volcanoes, are highlighted, together with the NW-SE trending lineaments (Pontine escarpment, Palinuro smt-Poseidon ridge, and the Tacito escarpment) acting as transfer faults. In the left box, location of sections A and B (Figure 14).

The aim of this work is to highlight the tectonic framework of this still poorly constrained area of the central-eastern Italian margin, i.e., the Pontine escarpment, and to sketch the evolutionary stages of the Tyrrhenian Sea back-arc basin taking into account the role of this particular area in the stepwise migration of the subduction system.

2. Geological Setting

2.1. The Tyrrhenian Abyssal Plain: Vavilov and Marsili Basins

The Vavilov basin has a roughly triangular shape, bordered to the southeast by the peninsular margins of Italy and to the west by the Sardinia margin (Figure 2); the latter is separated from the Vavilov abyssal plain by the Selli Line (Figures 2 and 3), a NE-SW trending fault scarp, that corresponds to a large-scale east dipping listric fault, flattening at depth along subhorizontal reflectors located close to the Moho, according to *Sartori et al.* [2004].

The seafloor is partly flat, more than 3000 m deep, and the basin is filled with distal turbidites deposits [*Gamberi and Marani*, 2004]. Several seamounts, ridges chains, and fault scarps complicate the seafloor morphology (Figure 3); in particular, the Magnaghi volcano is located west of the Selli Line, with a length of about 25 km and an elevation of 1470 m above the surrounding seafloor; it is made up of tholeiitic to alkali basalts [*Robin et al.*, 1987; *Savelli*, 1988] of late Pliocene age [*Savelli*, 1988; *Kastens and Mascle*, 1990]. In the central portion of the basin the Vavilov volcano is located, standing 2800 m above the seafloor and elongated in a NNE-SSW direction (Figure 3); it shows a steep, smooth western flank and a gentler eastern flank, and it is formed by tholeiitic to alkali basalts [*Robin et al.*, 1987; *Savelli*, 1988] of late Pliocene age [*Savelli*, 1988; *Kastens and Mascle*, 1990].

The northern apex of the Vavilov basin closes against the steep continental slope of the Latium-Campania margin. This area is bounded to the east by the prominent Flavio Gioia structural high and to the west by

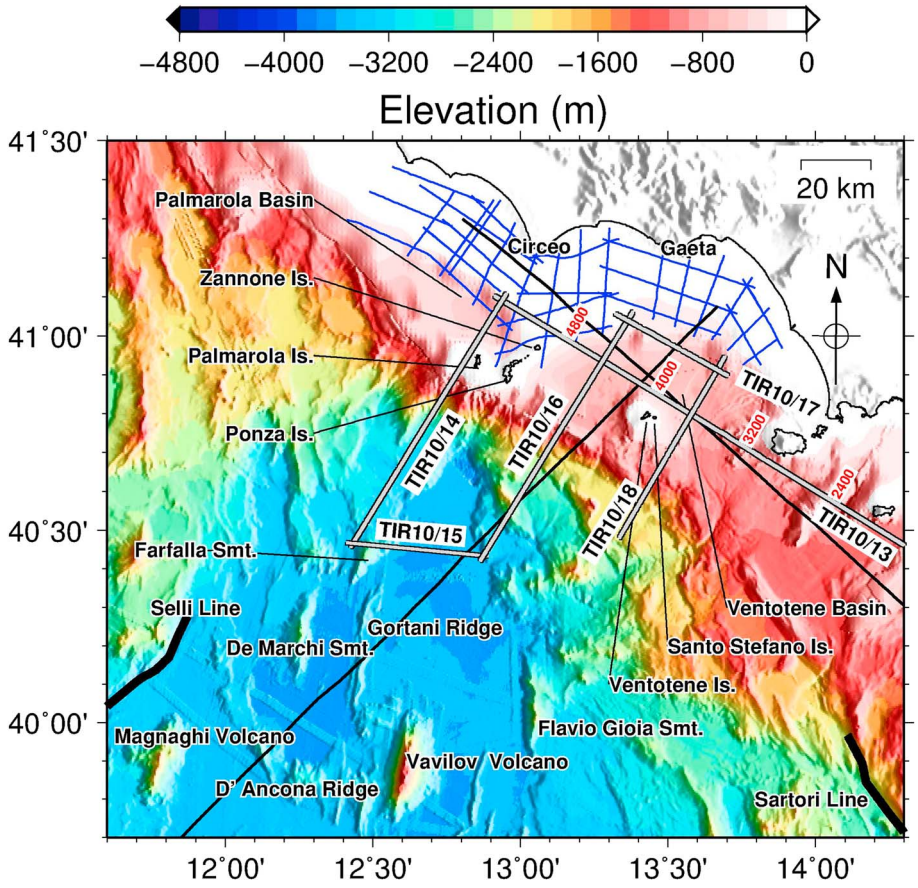

Figure 3. Bathymetric map of the Vavilov basin and of Latium-Campania Tyrrhenian margin, showing the main seamounts, ridge chains, and fault scarps interesting the seafloor morphology. The seismic data set analyzed in the study is displayed: the gray lines correspond to the TIR-10 survey; the blue lines are the "Reconnaissance seismic campaigns of the offshore areas" (zone E) of the Italian ViDEPI project, CROP survey in black lines.

the De Marchi high and the Farfalla seamount (Figure 3); the latter two features, the Flavio Gioia and De Marchi continental highs, both N-S trending and rising about 1200 m above the abyssal plain, are 80 km apart and are characterized by asymmetric flanks, with one of the latter dipping toward the basin steeper than the other. Between these two continental highs, the Gortani Ridge, a 40 km linear morphological high with an average elevation of 300-400 m, is made up of MOR basalts [*Beccaluva et al*., 1990]. Another relevant morphological feature is the D'Ancona Ridge, made up of several highs arranged in an arcuate shape.

The Issel swell, a thick crustal saddle, separates the Vavilov basin from the Marsili basin, located to the SE (Figure 2). The latter has a roughly elliptical shape with the flat 3500 m deep seafloor interrupted by the Marsili volcano, rising more than 3000 m from the surrounding plain. The NNE-SSW trending volcanic edifice is 60 km long and 20 km wide and is characterized by steep flanks [*Marani and Trua*, 2002]; NNE-SSW faults generate horst and graben structures bordering the seamount major axis.

The tectonic extension in the Tyrrhenian back-arc basin is linked to the eastward migration of the Apennines-Calabrian subduction system [*Malinverno and Ryan*, 1986]; according to *Doglioni et al*. [2004] and *Carminati et al*. [1998], the direction of extension in the northern part of the basin changed progressively from east to northeast, whereas in the southern part it changed from east to southeast. Furthermore, stretching was larger in this latter portion, where subduction of the old oceanic Ionian crust under the Calabrian arc still occurs. According to several authors [*Mascle and Rehault*, 1990; *Faccena et al*., 2001; *Sartori et al*., 2004; *Scrocca et al*., 2012; *Buttinelli et al*., 2014], this larger finite extension rate led to a fully continental breakup in some portions of the Tyrrhenian Sea, which are floored with oceanic crust; the emplacement developed during two distinct episodes: the oldest one is dated between 4.6 and 2.3 Ma, and it refers to the Vavilov

back-arc basin. The younger is dated less than 2 Ma and occurs in the Marsili back-arc basin, toward the southeastern portion of the Tyrrhenian Sea.

A strong asymmetry affects the conjugate margins of the Tyrrhenian Sea, represented by the eastern Sardinia continental margin and the central-southern Italy. According to several authors, an east dipping low-angle crustal detachment fault controlled the rifting process [*Mascle and Rehault*, 1990; *Jolivet et al*., 1998; *Sartori et al*., 2004; *Milia et al*., 2013]; the Sardinia passive margin represents the lower plate of the detachment system, whereas the Italian margin represents the upper plate. According to these interpretations, the asymmetric nature of the conjugate margins extends down to the Moho depth, which has been inferred at about 10 km.

2.2. Central-Eastern Tyrrhenian Margin

In the study area the continental shelf (delimited by the −200 m isobath) is around 25 km wide; it reaches its maximum extension offshore Circeo Promontory (more than 40 km of width) determining a structural high between the onshore portion and the western Pontine archipelago (Ponza, Zannone, and Palmarola Islands) (Figure 3).

The Circeo Promontory-Zannone alignment divides two major intraslope basins, which are the principal areas of sedimentary deposition in this area: the Palmarola basin, located to the NW of the alignment, has a maximum depth of 570 m and the thickness of the Plio-Quaternary sedimentary infill is about 1200 m [*Zitellini et al*., 1984]; the Ventotene basin, located to the SE, reaches a maximum depth of 860 m with a 1000 m thick Plio-Quaternary sedimentary sequence [*Zitellini et al*., 1984] (Figure 3).

Volcanic activity was very strong in the Latium-Campania margin during Plio-Quaternary time and is generally ascribed to the Roman province system [*Lustrino et al*., 2011, and references therein]. In particular, the western islands of the Pontine archipelago, i.e., Ponza, Palmarola, and Zannone Islands, are located on the structural high that divides the Ventotene and Palmarola basins, representing in fact an emerged part of the Tyrrhenian continental shelf; they developed during two main volcanic cycles of early Pliocene and Pleistocene age that produced submarine (rhyolite to rhyodacite) and subaerial (trachytic) acidic products. The eastern group of Pontine islands, Ventotene and Santo Stefano, represents the subaerial portion of a large submerged stratovolcano emplaced at the center of the Ventotene basin and rising about 700 m from the sea bottom; such islands are composed of basaltic to trachytic effusive and pyroclastic products [*Metrich et al*., 1988]. According to *Barberi et al*. [1967] and *Savelli* [1984, 1987] Ponza volcanism started at 5 Ma; *Cadoux et al*. [2005] indicated instead a starting date at 4.4 Ma, with the rhyolitic dykes and hyaloclastite deposit erupted in less than 500 ka. The trachytic bodies were emplaced between 1.3 and 1 Ma depending on the authors [*Barberi et al*., 1967; *Bellucci et al*., 1997; *Cadoux et al*., 2005], and they represent the end of the activity in this portion of the Pontine archipelago. The island of Palmarola was entirely built during the Early Pleistocene, with K-Ar ages ranging from 1.64 to 1.52 Ma, whereas volcanism at Ventotene and Santo Stefano erupted in a time span of 0.92–0.33 Ma [*Metrich et al*., 1988].

The volcanic products lie on a complex substratum, extensively exposed along the adjacent mainland and to minor extent at Zannone Island. It is composed generally by Apennine tectonic units made up of Meso-Cenozoic basinal or platform carbonates, overlain by terrigenous sequences of limestones and dolostones of Triassic age and by low-grade metamorphic units (Paleozoic?) cropping out at Zannone Island [*De Rita et al*., 1986], all stacked during the Apennine orogenesis.

Extensional processes occurring at the back of the eastward migrating Apennine subduction (previous section 2.1) affected the central-eastern Tyrrhenian margin since the upper Miocene [*Jolivet et al*., 1998]. This process gave rise to a general setting of asymmetric horsts and grabens, the latter filled by synrift and postrift siliciclastic deposits (conglomerates, sands, and shales) of marine, coastal, and deltaic environment [*Mariani and Prato*, 1988; *Cavinato et al*., 1994]. The changes in depositional environments caused the formation of several regional unconformities within the sedimentary infill of the basins [*Bartole*, 1984]. Extension mainly occurred along NW-SE normal faults, locally interrupted by NE-SW transverse structures characterized by a complex kinematics [*Acocella and Funiciello*, 2006; *Vignaroli et al*., 2016].

Extension displays a NW-SE-migrating pattern, inferred by the age of the sedimentary infilling of the marginal basins. In the western Tuscany area, extension took place since middle Miocene, and several NW-SE oriented basins formed [e.g., *Bartole*, 1990; *Pascucci et al*., 1999, 2006; *Cornamusini et al*., 2002; *Brogi et al*., 2014. During

the late Messinian a relative quiescence time took place in the area, according to *Pascucci et al*. [1999], followed by a new extensional stage in early Pliocene; a post rift phase occurred in late Pliocene. Offshore the northern Latium, first events of basin formation occurred since late Tortonian, according to *Bartole* [1990], or even during early to middle Miocene, according to *Buttinelli et al*. [2014]. In the southern Latium region, the structural depression of the Pontina Plain is controlled by a SW dipping normal fault and the oldest basin infill is lower Pliocene in age [*Bellotti et al*., 1997]. Along the Campania margin, south of the Aurunci Mountains, the main coastal basins are the Garigliano plain, the Campania plain, and the Sele Plain; in this part the extensional phase acted mainly through NE-SW transverse normal fault systems and took place from late Pliocene to Quaternary times [*Billi et al*., 1997; *Aiello et al*., 2011].

Volcanic activity along the eastern Tyrrhenian margin shows a similar spatial and temporal SE migrating pattern (Figure 1). The Tuscan margin is characterized by acidic intrusive and volcanic products with associated high-temperature metamorphism [*Acocella and Rossetti*, 2002; *Rossetti et al*., 2008]. The oldest products are lamproitic rocks occurring as dykes, of middle Miocene age (~14.2 Ma [*Civetta et al*., 1978]); the following activity is dated late Miocene (~8.5–5 Ma) and characterized by granitoid intrusions and minor volcanic potassic to ultrapotassic, whose products have been dredged from the Tuscan Archipelago (Elba, Capraia, Montecristo, and Giglio Islands [*Peccerillo*, 2005; *Lustrino et al*., 2011, and reference therein]. The latest products are Plio-Quaternary basic to acid intrusive and eruptive products, in northwestern Tuscany (e.g., Montecatini, Val di Cecina, Larderello, Roccastrada, Mount Amiata, Radicofani, and Torre Alfina) and northwest Latium (Tolfa, Manziana, and Cerite) [*Lustrino et al*., 2011, and reference therein]. Along the Latium-Campania margin volcanic activity spanned from Pliocene to Present; the oldest activity began at Ponza Island, as described in details before in this section. A second important volcanic episode is late Pliocene (~2 Ma) and took place northwest of Naples, with andesites and basaltic andesites [*Barbieri et al*., 1979]; the main phase of magmatic activity is early Pleistocene and continues until recent time [*Peccerillo*, 2005, and references therein]. The Roman Province (~0.8–0.04 Ma) includes the large stratovolcanoes and volcanic complexes of Vulsini, Vico, Sabatini, and Alban Hills, which erupted mafic to felsic rocks belonging to the potassic series and to the highly potassic series [*Peccerillo*, 2005]. Moving toward the south, products from Ernici-Roccamonfina volcanoes are dated ~0.7–0.1 Ma, whereas over the last 0.3 Ma a voluminous ignimbrite activity started in the Campanian Plain and Naples Bay [*Milia and Torrente*, 2007] and lasted until present times.

All the above suggests that extensional basins and arc-related volcanism along the Tuscany-Latium-Campania margin migrated progressively from NW to SE in the Tyrrhenian domain, together with slab rollback and subduction hinge retreat.

The extensional phase played a major role also in the physiographic setting of the escarpment connecting the shelf to the abyssal plain. The shelf break is well defined and segmented, with a variable depth between 95 and 160 m, deeper between Ponza and Palmarola islands. Beyond the shelf break a very steep, NW-SE trending continental escarpment is present. Close to the western Pontine Archipelago, a single slope escarpment is responsible for the deepening of the margin toward the Vavilov plain; in this portion it is the steepest continental slope of the Eastern Tyrrhenian continental margin, with inclination locally up to 30° [*Chiocci and Orlando*, 1996]. It has a very complex morphology, with erosive/instability phenomena affecting almost all (98%) of the continental slope seafloor facing the Western Pontine Archipelago and causing slope retreat [*Chiocci et al*., 2003]. Toward the southern region, the escarpment constantly widens and a set of closely spaced fault scarps develops in a NNW-SSE direction, resulting in a downthrown stepping margin morphology (Figure 2); they follow the trend of the so-called Sartori escarpment, a major fault system [*Curzi et al*., 2003], 80 km long, interpreted as a left-lateral transtensive system [*Musacchio et al*., 1999]. Due to the recent age of tectonic events that created this setting, the basement highs are not yet mantled by slope sediments; so, the main loci for sediment accumulations are the intraslope basins formed over the basement depressions, generally NNW-SSE trending. These basins are narrow, and some portions are characterized by drainage systems that connect successive deeper basins, until the abyssal plain. The upper part of the continental slope ($<$2000 m depth) hosts numerous, relatively short, fault scarps, which dissect the region into different small horsts and grabens, trending N-S and NE-SW.

The offshore seismicity of the Central-Eastern Tyrrhenian margin is characterized by a weak activity, even if small earthquakes are more frequent here than onshore [*Favali et al*., 2004].

Through the proposed interpretation of new multichannel seismic profiles, we better investigate the evolution of this complex part of the eastern Tyrrhenian margin. We especially focused on the poorly documented geometry and kinematics of normal faults, considering that the proximity to the Vavilov basin makes this area representative of the transition from a continental to a back-arc crust with oceanic affinity.

3. Data and Methods

3.1. Seismic Data Acquisition and Processing

Cruise TIR-10, funded by Consiglio Nazionale delle Ricerche (CNR) of Italy in the frame of the Italian CROP (CROsta Profonda) Project [*Scrocca et al.*, 2003a, 2003b; http://www.crop.cnr.it], was carried out in the Tyrrhenian Sea in October 2010 (TIR-10 cruise report available at http://www.ismar.cnr.it [*Doglioni et al.*, 2012]).

Five new multichannel seismic reflection lines, located along the Latium-Campania margin (Figure 3), have been acquired and processed. Subsequently, the major unconformities and structural features have been interpreted in order to recognize the main morpho-structures displayed in the area. The new data set has been calibrated with deep well logs and integrated with the reappraisal and critical review of a large amount of literature data.

The research cruise was carried out with the 61 m R/V *Urania*, a ship normally used for geological, geophysical, and oceanographic work; during the survey, a total of 1006 km of multichannel reflection seismic lines were acquired, together with 100 km^2 of multibeam and 1000 km of Sub Bottom Profiling.

The seismic source used was a tuned array of three SERCEL's GI-GUN, configured in harmonic mode (983.2 + 983.2 cm^3, 983.2 + 983.2 cm^3, 737.4 + 737.4 in^3), with an operative pressure of 2000 psi (140 bar) and towed at 5 m. The cable used in the acquisition was a SERCEL digital streamer, 1225 m long, composed by 97 channels with a group interval of 12.5 m, towed at 4–7 m depth. There were two channel units: a shorter one composed of one channel group, and lying behind the source, devoted to acquire auxiliary data, such as the signature; a longer one, for seismic data recording, composed by 96 channels. The recording trace length was 12 s, shot interval was 37.5 m, and the seismic sampling rate was 0.5 ms.

The complete TIR-10 survey is composed by 20 lines; for this study, focused on the Latium-Campania margin, lines from TIR10-13 to TIR10-18 were processed and interpreted, for a total length of about 350 km. Three lines have a NW-SE orientation (parallel to the Italian coast); the others are perpendicular (NE-SW); they investigate part of the continental platform, the continental slope, and part of the abyssal Tyrrhenian plain up to 3500 m of depth (Figure 3).

The processing sequence applied to the seismic raw data [*Yilmaz*, 2001] is here briefly resumed, and it is the result of several tests and evaluations. Data processing consists in a sequence of operations aimed to enhance the signal/noise ratio and to display the results in the form of a seismic section, in order to obtain geological information from it. The software package "2D Promax" (Hulliburton) was used for the basic processing procedures, aimed at generating poststack time-migrated sections ready for interpretation.

In the preprocessing stage, field geometry was assigned to the seismic trace with the aim of storing coordinates of shot and receiver locations on the trace headers; then, top mute was used to remove noise above the first arrival and direct waves, and trace kill was applied to delete noisy traces. In order to suppress the strong swell noise affecting the data, a low-frequency band-limited noise-suppression filter was used; a gain recovery function followed, in order to compensate the spherical divergence effect. The following step was to apply the predictive deconvolution, which is a fundamental tool in the elaboration of seismic data, allowing the improvement of the temporal resolution of the data and to attenuate multiple reflections. Once the traces were sorted on common depth point gathers, the next step was the velocity analysis, an essential tool in order to apply the normal move out correction and to produce the first stacked seismic section. Two different methods were used: first, a velocity analysis with the constant velocity scan method was carried out. A second velocity analysis was carried out with the semblance method, and the velocity field obtained, after some smoothing, was used to produce the final stack section. Kirchhoff migration resulted to be the most efficient algorithm among the different types of migration algorithms tested in the post stack processing phase. Besides this basic processing sequence, some other processes were applied (radon velocity analysis, tau-p transform, and F-K filter) in order to improve the signal/noise ratio.

A network of seismic lines acquired in 1986 by Western Geophysical Co. for the Agip oil company (Zone E) has been taken into account, along with the new seismic profiles. These lines constitute a public data set available in the framework of the ViDEPI Project (www.videpi.com), and they mainly investigate the shallower continental platform area. Part of the two CROP profiles crossing the area, M-29B and M-36, complete the seismic data set used in this work. In this paper only the interpretation and results from the new seismic lines are presented, although also the interpretation of both the CROP and the Zone E lines contributed to unravel the general setting of the area (Figure 3).

Seismic interpretation was carried out identifying the main seismic unconformities and units and trying to calibrate them using the information provided by exploration wells and Ocean Drilling Program (ODP) sites, as well as comparing lithologies with those outcropping in the mainland.

3.2. Magnetic Data

During the TIR-10 cruise, a Seaspy marine magnetometer was towed 180 m astern of the R/V *Urania*, simultaneously with the seismic reflection acquisition. Raw magnetic data were sampled at 1 Hz by using the Marine Magnetics Sealink software, and the positioning of the magnetic tow-fish was assured by the FUGRO differential GPS coupled with the lay-back-correction performed in real time by the Sealink software. The depth of the magnetometer has been roughly constant during the navigation and steadily monitored. Total-field magnetic data were processed by removing spikes and diurnal variations using the INGV reference stations of Duronia and L'Aquila. Magnetic anomaly field has been calculated by removing the International Geomagnetic Reference Field (IGRF2010 http://www.ngdc.noaa.gov/IAGA/vmod). A statistical leveling procedure was applied to the data in order to minimize the crossover errors evaluated at the intersections between magnetic lines and to produce a smoother distribution of the magnetic anomalies.

Concerning the complex origin of the rocks of this area, high remnant magnetization contribution may be plausible. Moreover, because of the impossibility to grid the data coming from five lines, the reduction to the pole has not been applied. A phase shifting between the magnetic anomalies and the relative causative sources may be present in the profiles.

4. Seismic Stratigraphy and Chronostratigraphy

A chronostratigraphic calibration of the seismic profiles was attempted by using data provided by some exploration wells located along the Latium-Campania coast and offshore, and ODP sites, Leg 107 [*Kastens et al*., 1988] drilled in the Vavilov plain.

Wells are used in this work for indirect calibration of the seismic lines, in order to have a qualitative idea of the subsurface geology in the area (Figure 4 for location and Figure 5 for stratigraphy). Two offshore wells (Michela 1 and Mara 1) are located on the continental shelf, near the Italian coast. Michela 1 well, which drilled a total depth of 2552 m, is located offshore between Anzio and Capo Circeo, where Mara 1 well, located in the Gaeta Gulf, reached the depth of 2910 m (Figure 4) (http://unmig.sviluppoeconomico.gov.it/videpi).

Regarding the abyssal area, the stratigraphic knowledge is mainly based on the seven sites of the Ocean Drilling Program (ODP), Leg107, drilled across the Tyrrhenian basin; sites 651 and 655 are the closest to the area object of this study and their information [*Kastens et al*., 1988] was used to tentatively calibrate the new seismic data in their deepest portion (Figure 4).

The main unconformities have been interpreted according to the seismo-stratigraphic units of the Tyrrhenian Basin defined in previous works [*Zitellini et al*., 1984; *Moussat et al*., 1986]. Based on all the available data, four main seismic units have been identified (named U1, U2, U3, and U4), delimited by three main unconformity surfaces (named A, B, and C) (Figure 5).

Seismic Unit U1 (Mesozoic-Cenozoic) is the lowest seismic unit identified, characterized by a scarce penetration of the seismic signal; it generally displays an undifferentiated seismic facies, but where reflections are visible, they display variable amplitude and frequency and are mostly discontinuous and chaotic, indicating lack of stratification (Figure 5, U1 unit). Probably, the presence of compressive structures involving this unit is the main reason for the low quality of the data, caused by internal reflection disturbances. The horizon A at the top of unit U1 generally reflects the major part of the seismic energy and appears discontinuous (Figures 6 and 7); this unit can be considered the acoustic substratum of the area. U1 unit has been correlated

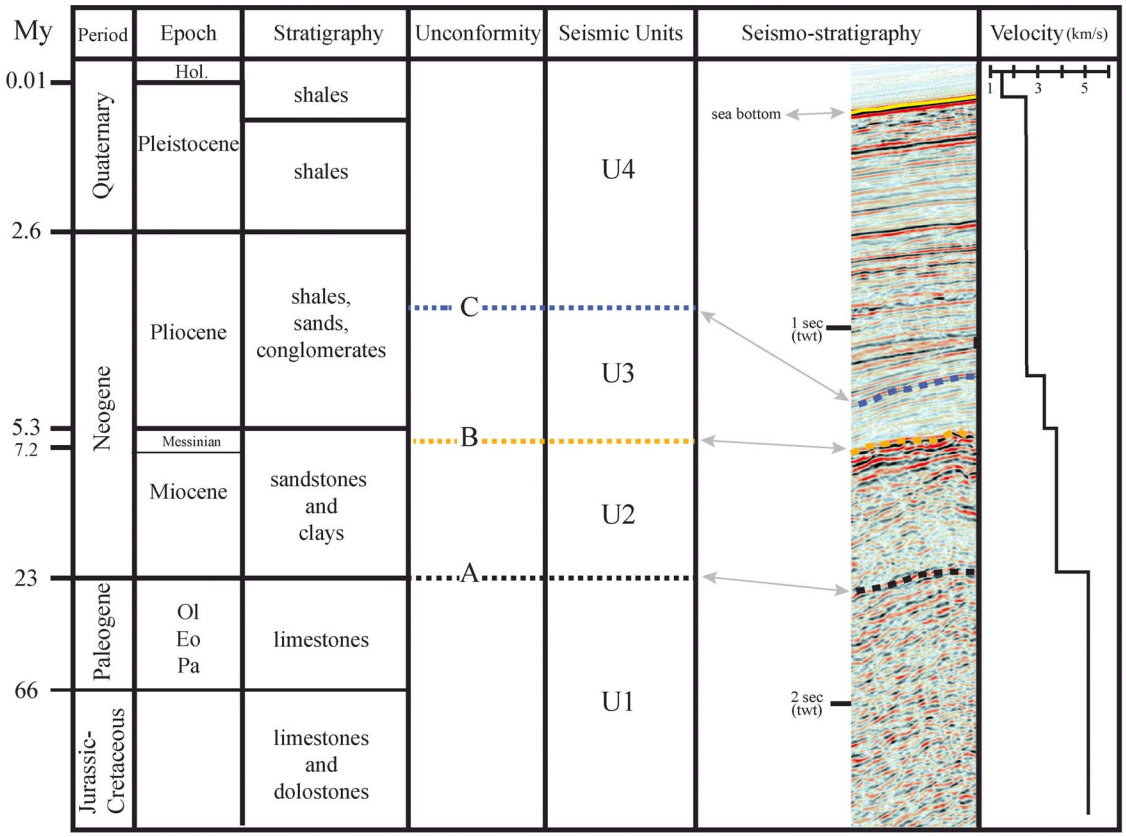

Figure 4. (a) Schematic stratigraphy and correlation of exploration wells Michela 1, Mara 1, and ODP Site 651A (blue on location map). (b) The map shows the location of exploration wells in the study. Offshore wells: Michela 1, Mara 1. Onshorewells: Latina 1 (Lt1), Latina 2 (Lt2), Acciarella (Ac), Fiume Astura (FA), Tre Cancelli (TC), Fogliano (Fo), Cellole Aurunci (CA), Mondragone (Mo), Castelvolturno 1,2,3 (Cv 1,2,3), Grazzanise (Gr), Cancello 1,2 (Ca 1,2);Apramo (Ap), Villa Literno 1 (VL), Qualiano (Ql). ODP sites 652A and site 655B.

to the Meso-Cenozoic carbonates, widely cropping out in the near onshore areas, in the Lepini and Aurunci massifs the Massico Mountain, Zannone Island, and Circeo Mountain. Moreover, limestones correlated to unit U1 are drilled offshore, in both Michela 1 and Mara 1 wells, at a depth of about 2100 m and 1500 m, respectively.

Seismic unit U2 (Miocene) is characterized by a chaotic seismic facies, with scattered discontinuous reflectors, medium amplitude, and variable frequency, indicative of heterogeneous lithologies (Figure 5, U2 unit). As inferred by the outcropping geology of the Latium-Campania regions, this unit can be correlated with the Miocene flysch deposits and other, more internal, siliciclastic units (Flysch of Frosinone and Flysch of Cilento) [*D'argenio et al*., 1973; *Parotto and Praturlon*, 1975]. Some of the exploration wells drilled Miocene deposits like Mara 1 (1220 m of depth), Michela 1 (1574 m of depth), Fogliano 1 (410 m), Cellole Arunci 1 (1220 m), and probably Mondragone 1 (700 m); generally, the Miocene succession is made of clays and sands, with locally interbedded conglomerates. Unit U2 constitutes, together with the previous one (U1), the substratum of the area; it is not well displayed in all the seismic data sets, and it seems to be absent in the structural elevated areas where the substratum is composed only by the Meso-Cenozoic calcareous deposits (Figure 6, Shots 600–900). The lower unconformity (A) of the unit has already been described; the upper unconformity (B) is a strong reflector, characterized by a high amplitude and strong impedance contrast (Figures 6 and 7, and following); it is well visible in all the data set, although sometimes, it is formed by several diffraction hyperbolas, more than a single and well-defined seismic horizon. This unconformity has a regional importance, being linked to the top of the evaporites deposited during the late Messinian salinity crises or to an erosional unconformity formed during the late Messinian sea level drop [*Malinverno*, 1981]; sometimes, erosional truncation geometry of the unit U2 on this unconformity has been observed.

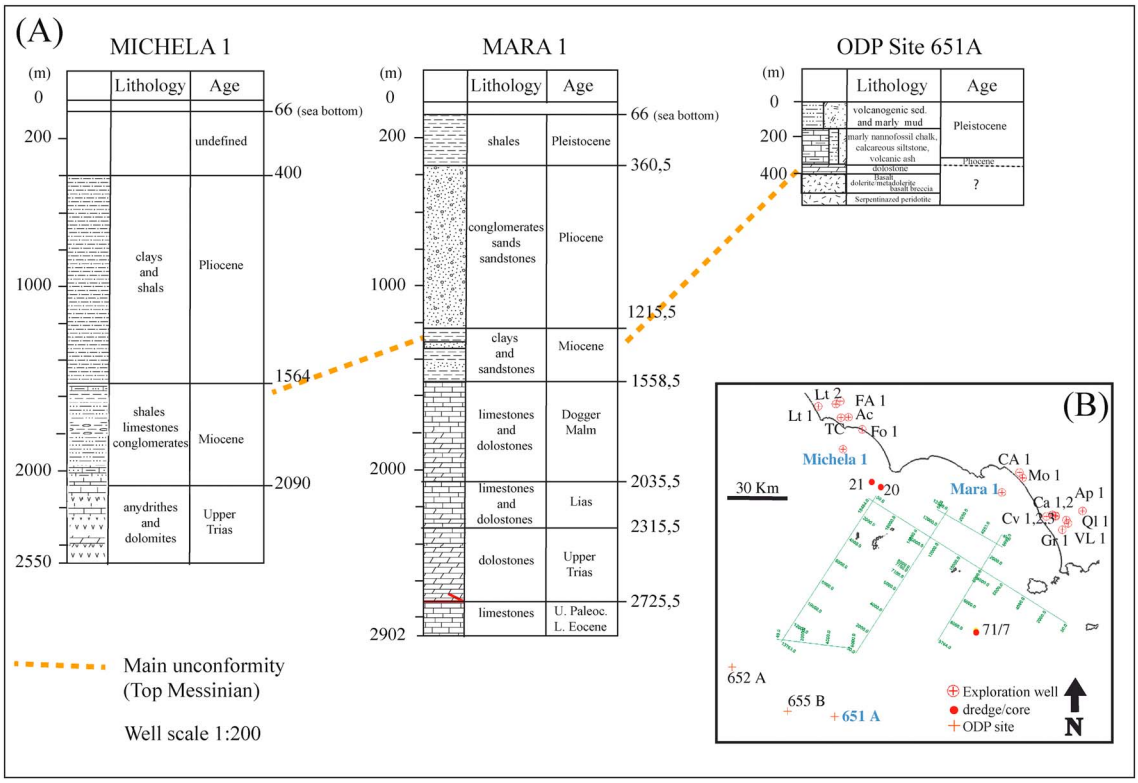

Figure 5. (a–c) Seismostratigraphic units (U1–U4) and unconformities recognized in the offshore area of Latium-Campania margin in this work. Correlation between stratigraphy, seismic units, and seismic velocities is based on seismic facies analysis, lithostratigraphic data from wells close to the investigated area, and velocity data from literature [*Prada et al*., 2014] and processing procedure (stacking velocities). (U1: Mesozoic-Cenozoic, U2: Miocene, U3: early Pliocene–middle Pliocene p.p.; U4: middle Pliocene p.p. to Pleistocene; A: top Meso-Cenozoic; B: top Messinian unconformity; C: Middle Pliocene p.p. unconformity).

Seismic unit U3 (early Pliocene to middle Pliocene p.p.) lies upon the unconformity B that marks the top of the evaporitic Messinian; basal reflections inside U3 are generally parallel to the B horizon (Figure 8a), or they onlap it in presence of structural highs (Figure 9, Shots 4700–4500); locally, B also displays an erosive character. The upper boundary of the unit is generally a well-distinguishable surface, parallel to the upper reflectors of the unit. Internal reflections are generally continuous and well imaged, from low to medium amplitude, medium frequency, with a parallel to subparallel geometry and horizontal pattern; the overall unit shows wedge geometry, being thicker in the basin depocenters and progressively thinner in the proximity of the horsts that bound the basins (Figures 6a and 9, Shots 4400–4800). The time thickness of U3 varies due to the irregular morphology of the underlying unconformity, being maximum in the basin where it reaches about 1 s (twt) of thickness. In some parts (i.e., the deepest areas) it is possible to divide the U3 unit in a lower part ($U3_a$) formed by high-amplitude reflectors progressively becoming a transparent facies, with low amplitude and high frequency, probably associated with a more fine-grained clastic sediment. The overlain subunit ($U3_b$) is formed by continuous, well-layered reflections, with medium amplitude and high frequency. The subunit at the top ($U3_c$) is a thin sequence characterized by a higher amplitude of the reflections. According to the well analysis, unit U3 can be correlated with the Pliocene deposits drilled by almost all of the wells, which found a succession made in general of interbedded clays and sands, locally with intercalated conglomerates; these more coarse-grained sediments are detected on the seismic lines by stronger and less organized reflections. Depositional environment is marine, infralittoral according to *Ippolito et al*. [1973]. In some portions of the seismic lines normal faults with limited (or null, for seismic resolution) offset are detected in this unit, as well as evidence of folding (Figure 7a); this highlights tectonic activity during the deposition of this unit.

Seismic unit U4 (middle Pliocene p.p. to Pleistocene) is the uppermost seismic unit, divided from the underlying unit U3 by a basal unconformity here named C. This surface highlights an evident variation of the depositional geometries, marking the beginning of the progradation in the basin fill and locally the end of the tectonic activity (no evident deformation is displayed in unit U4). The internal reflection configuration

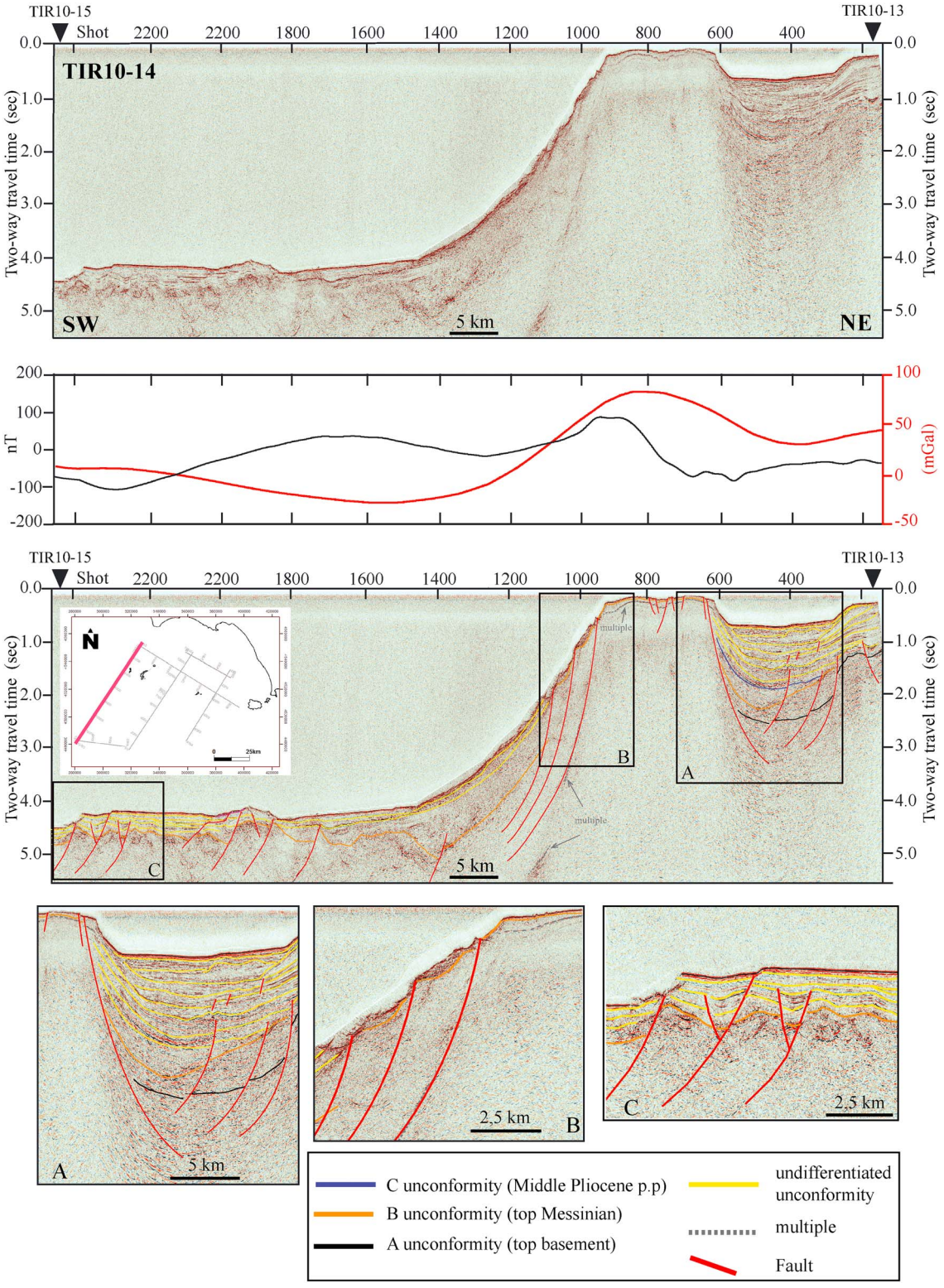

Figure 6. Kirchhoff time migrated seismic line TIR10-14, running NE-SW for about 85 km across the Latium margin and connecting the continental shelf to the Vavilov basin, in the area where the escarpment shows its maximum gradient and minor horizontal extension (location shown in the white box). (top) Processed data only, with magnetic data (this study) and satellite-derived free air gravity anomaly from *Sandwell and Smith* [1997]. (bottom) Interpreted processed data; symbols provided by the legend. Insets: (a) Detail focusing on the continental shelf area characterized by a main extensional fault dipping toward the mainland and dividing the Ponza-Palmarola structural high from the Palmarola basin. (b) The NW-SE fault system responsible for the lowering of the margin is shown; erosion/exposure of the substrate is predominant. (c) The abyssal area, with faults that clearly offsets the seafloor and mild folds suggesting a possible transtensional deformation.

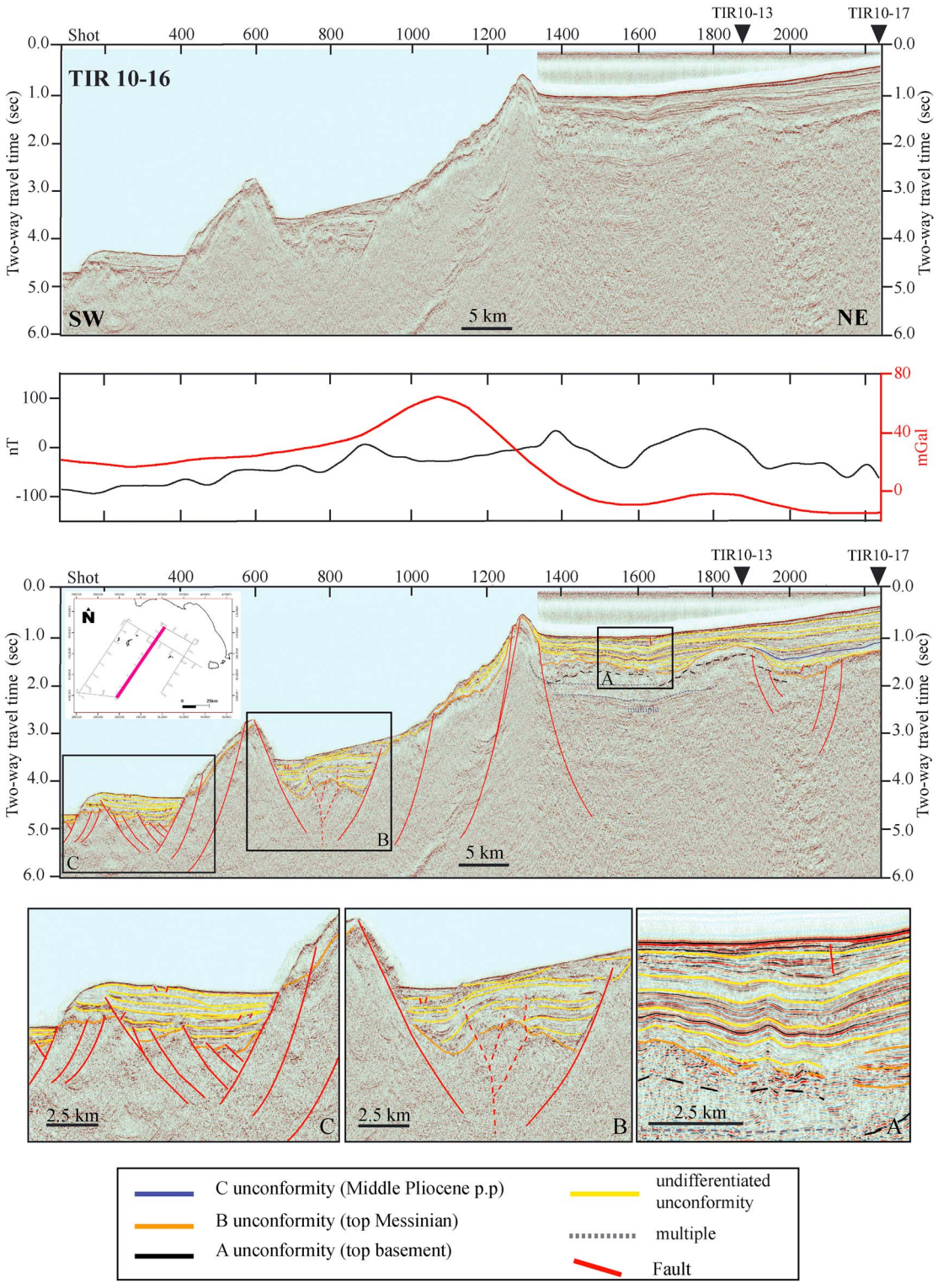

Figure 7. Kirchhoff time migrated seismic line TIR10-16, running NE-SW for about 85 km across the Gaeta gulf to the Vavilov basin, north of Flavio Gioia continental high (location shown in the white box). (top) Processed data only, with magnetic data (this study) and satellite-derived free air gravity anomaly from *Sandwell and Smith* [1997]. (bottom) Interpreted processed data; symbols provided by the legend. Insets: (a) Detail focused on symmetric folds deforming the Plio-Pleistocene sedimentary cover on the continental shelf area, interpreted as related to strike-slip positive structures. (b) Basement depression at the base of the escarpment, bordered by a fault plane and showing a sedimentary infill organized in a syncline geometry; the geometry showed by the reflectors could be linked to strike-slip movements or alternatively to a gravity flow event originated from the margin to the NE. (c) In the abyssal area the basement is formed by minor tilted blocks covered by progressively thinner sedimentary cover. Recent fault activity is testified by the fault at the end of the line cutting the seafloor.

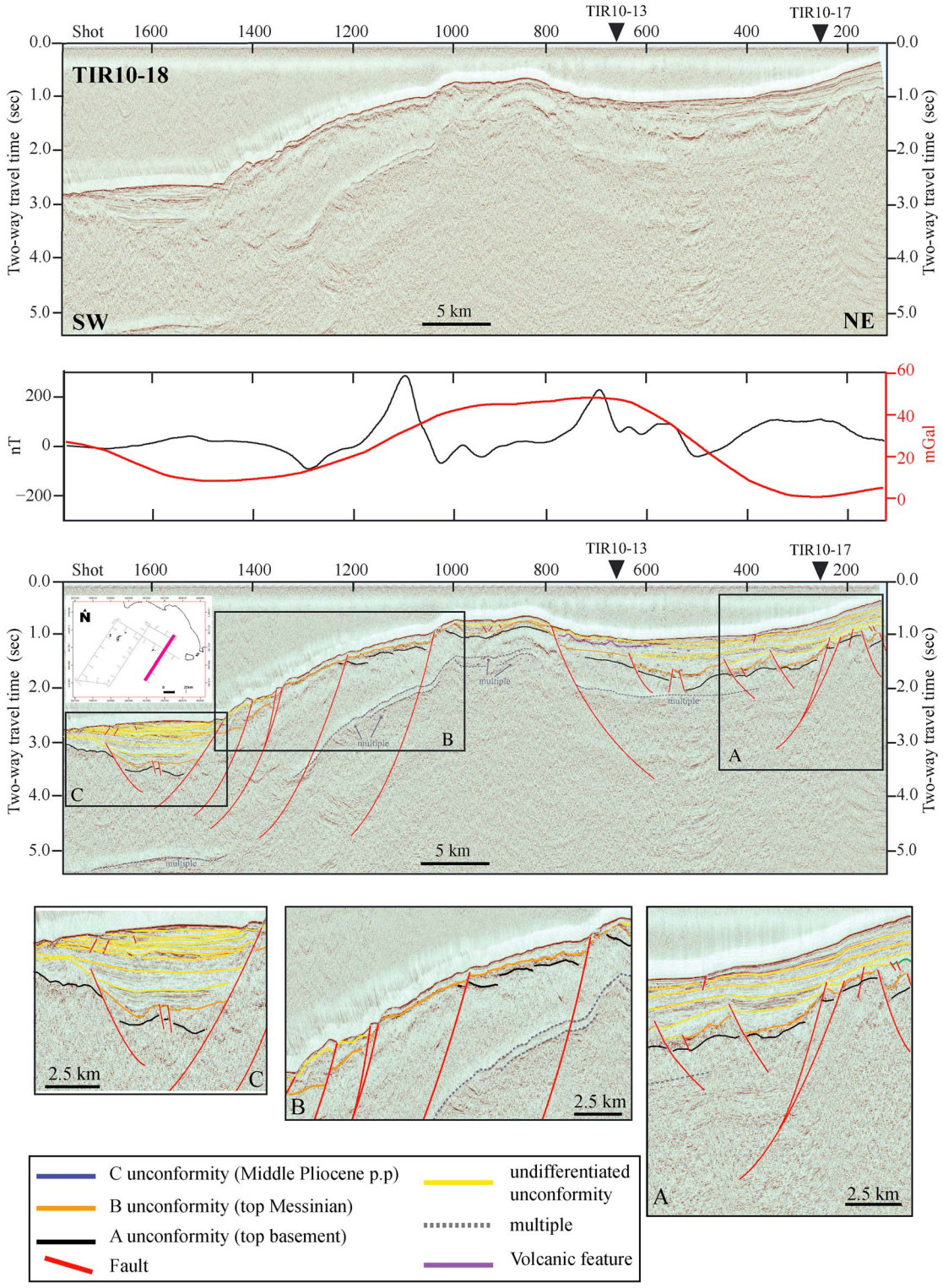

Figure 8. Kirchhoff time migrated seismic line TIR10-18, running NE-SW across the Ventotene basin between the Ventotene and Ischia islands (location shown in the white box). (top) Processed data only, with magnetic data (this study) and satellite-derived free air gravity anomaly from *Sandwell and Smith* [1997]. (bottom) Interpreted processed data; symbols provided by the legend. Insets: (a) Detail of the several extensional faults dissecting the Ventotene basin substratum, probably linked to the NE-SW system fault affecting this area toward the Ischia Island. The basin infill reaches a maximum a maximum thickness of 0.7 s (twt) and is formed by parallel and continuous reflectors. (b) Detail of the escarpment morphology south of Ventotene Island; widely spaced listric normal faults testified a less localized deformation respect to the northern part (Figure 5), and the result is a gentler morphology of the down-stepping margin. (c) Focus on a faulted basin at the bottom of the escarpment characterized by a sedimentary fill of almost 1 s (twt) of sediments.

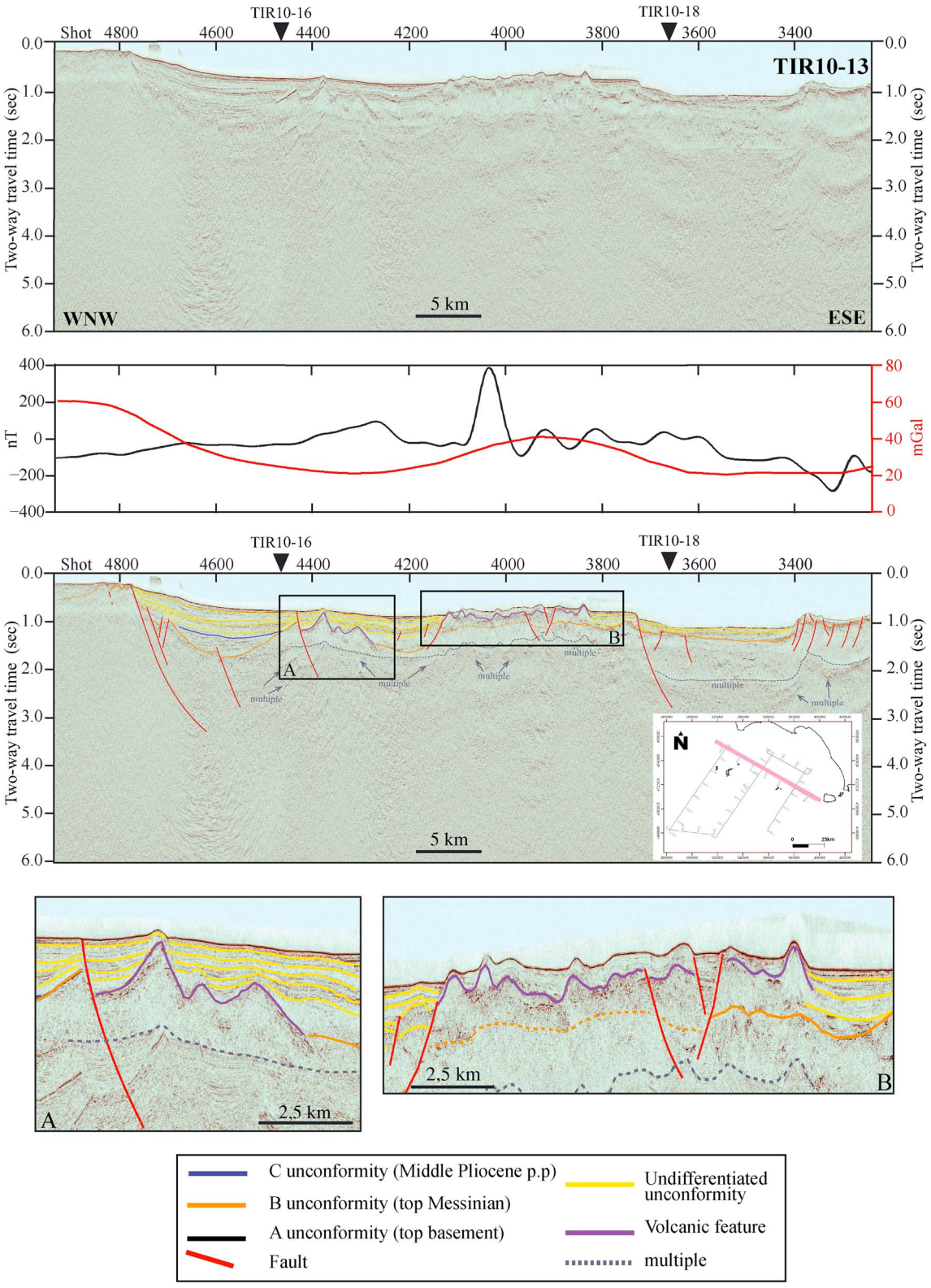

Figure 9. Kirchhoff time migrated seismic line TIR10-13, running parallel to the Latium-Campania margin (NW-SE) from offshore Circeo promontory to the Banco di Fuori and Ischia structural highs (location shown in the white box). (top) Processed data only, with magnetic data (this study) and satellite-derived free air gravity anomaly from *Sandwell and Smith* [1997]. (bottom) Interpreted processed data; symbols provided by the legend. Insets: (a) Detail of the Ventotene basin which results to be divided in two depocenters by a cone shaped structure whose origin is inferred to be volcanic. (b) Focus on several cone shaped features associated to the Ventotene volcanic complex.

of unit U4 on the continental shelf area consists in prograding clinoforms, probably of deltaic environment (Figure 6, Shots 100–300); on seismic profiles parallel to the direction of progradation, it is possible to recognize topset, foreset, and bottomset beds of sigmoidal or oblique clinoforms. The deltaic system was probably supplied during Pleistocene times by the adjacent Latium-Campania plains, and the main direction of progradation was basinward. Offlap breaks seem to move seaward, which indicate a regressive trend of the marine and coastal facies. Several main unconformities are observed within the unit U4; the bottom part of the reflections displays a slightly downlap termination on the basal unconformity surface, and then basinward they became concordant with it. In addition to the continuous, low to medium amplitude reflectors described above, localized and chaotic reflections probably due to slumping, especially in the proximity of structural highs of the basements, are also observed (Figure 6a, Shot 400, 0.5 twt). Cut and fillings of canyons or channels, sometimes in correspondence with modern channels, are also present. This unit is crossed by all wells present in the area; it can be noticed that the Pleistocene sequence shows very different thickness along the area, minimum in the northern area (around 1000 m), and maximum to the south (more than 3000 m), as already pointed out by the analysis of the well data. The analysis of the seismic facies and the information provided by the wells identify the sequence as composed essentially by conglomerates, sands and clays of deltaic environment, evolving to a more marine environment in the upper part of the sequence. A middle Pliocene p.p. to Pleistocene age is assumed for this sequence.

Volcanic unit (V) is an additional facies, included within the seismic unit U4; it is characterized by a low signal/noise ratio due to the scattering of the seismic energy due to the presence of volcanic rocks. It occurred especially in the central-eastern area along the line TIR10-13 as it approximates the Ventotene volcanic region (Figure 9b), and along the line TIR10-17, where some volcanic features are detected [*Cuffaro et al*., 2016], and in the NW part in correspondence with the Ponza high, whose substrate is probably of volcanic origin. The reflections appear chaotic, discontinuous, and with high amplitude.

The described seismic units were defined on the continental shelf; thus, additional considerations are required to define the seismic character of the sedimentary sequences along the continental slope and the Vavilov plain, which extends at the base of the escarpment. On the steep continental slope, a thin succession of reflectors is observed, lying upon a basal unconformity characterized by strong acoustic impedance with, in some cases, an erosive character (Figures 6b and 8b); the internal reflections show low amplitude and frequency, and sometimes a discontinuous pattern. Where the escarpment shows major dip, the sequence is absent. In some areas, chaotic facies are found, with discontinuous and disrupted reflectors, due probably to instability phenomena (Figure 7b), or bodies with mounded geometries and still visible internal reflections (Figure 7, Shots 1200–1100).

5. Seismic Interpretation

Seismic interpretation was carried out by using Petrel 2012.1 software (Schlumberger), which allows to manage digital seismic data in SEG-Y format and to represent the data set in a georeferenced environment; furthermore, three-dimensional visualization is an efficient tool in verify interpretation at the intersection of the lines, the horizons geometry, or the structural trends within the entire 2-D data set. In this paragraph the new seismic lines acquired will be described in detail. TIR10-14, TIR10-16, and TIR10-18 are NE-SW trending lines, about 30 km spaced, and they investigate the areas of the continental platform, the escarpment, and the proximal part of the Vavilov basin. TIR10-13 and TIR10-15 are NW-SE trending, parallel to the coast line, located respectively on the continental margin area, and in the northern part of the Vavilov basin facing the Pontine slope.

5.1. TIR10-14 Seismic Profile

The seismic line TIR10-14 extends for a length of about 85 km in a NE-SW direction; it starts on the edge of the continental shelf, offshore Circeo promontory, and crosses the Palmarola basin east of Palmarola Island, continuing until the Farfalla seamount (Figures 3 and 6).

Prograding units from the continental shelf are imaged on the NE portion of the line; they extend basinward, filling the Palmarola basin ahead. The maximum thickness of the sedimentary infilling is in the order of 1.5 s (twt), and three main unconformities are recognized by means of correlation from seismic profiles of the E survey: the lower unconformity correspond to the top of the Messinian unconformity (B unconformity,

orange) and shows a variable depth between 1 and 2.2 s (twt), deepening seaward. Above the U2, that onlaps onto the unconformity B, mid-Pliocene-Pleistocene sequence displays two unconformity surfaces dividing parallel reflectors below and the progradational sequence above. The main extensional fault controlling the basin development dips toward the mainland and bounds the Palmarola-Ponza structural high; it shows a throw of more than 1 s (twt) (in the order of 1 km) and its activity lasted from late Messinian-Early Pliocene to recent times (Figure 6a). Minor extensional faults dissected the basin substratum, with small displacements (0.1–0.2 s twt), affecting the basal part of the early Pliocene sequence (U3) and progressively abandoned upsection.

The Palmarola basin is bordered seaward by the Palmarola-Ponza High (Shots 580–890), where the seafloor is located around 0.1 s (twt). The strong reflectivity of this horizon let to infer the presence of a hard substratum that could be linked to the occurrence of volcanic products of Ponza and Palmarola or of the Meso-Cenozoic carbonate basement. This interpretation is supported by the outcropping of Paleozoic metamorphic and Meso-Cenozoic sedimentary units in the close Zannone Island. The Palmarola-Ponza high, bounded by normal faults, separates the Palmarola basin from the adjacent Ventotene basin. NE-SW en echelon trending normal faults affects the margins of Palmarola-Ponza high, producing the lowering to the Ventotene basin southeastward and, less abruptly, northwestward to the Palmarola basin [*De Rita et al*., 1986].

Offshore Palmarola Island, line TIR10-14 crosses the main escarpment which shows here its minimum width, around 15 km, and maximum slope gradient, locally up to 30°. It is structurally controlled by a normal fault system, NW-SE trending, responsible for the lowering of the margin down to the deep abyssal plain at 3500 m of depth. The upper part shows a predominance of erosional features and exposure of the basement (Figure 6b); this fact and the pronounced steepness can mask the nature of the escarpment to the seismic prospecting, and no reflections are visible. The high gradient, typical of the upper continental slope and ridge flanks, triggers huge instability/erosive phenomena, such as linear scar-channel systems, dendritic gullies networks, canyons, and simple or complex slides. As a consequence, a cannibalization of the slope is observed [*Chiocci et al*., 2003]. In the lower part of the escarpment, where the gradient is less extreme, TIR10-14 profile shows a continuity of the reflectors packages toward the flat area; the thin and localized sedimentary cover shows chaotic and discontinuous internal reflections, with variable amplitude and frequency. This lower gradient area is characterized by sedimentation, such as mass flow located inside the wide valleys carving the continental slope [*Chiocci et al*., 2003].

In its final part, TIR10-14 crosses the area of Farfalla seamount, where several extensional faults are observed, together with gentle folds, suggesting possible transtensional deformation; in some cases faults clearly offsets the seafloor (Figure 6c).

5.2. TIR10-16 Seismic Profile

Line TIR10-16 has a NE-SW trending, it starts on the edge of continental shelf in the area of the Gaeta Gulf and it ends on the eastern margin of the northern apex of the Vavilov basin, north of Flavio Gioia high. It has a total length of 85 km and crosses the intraslope basin of Ventotene, between the western Pontine Islands (Ponza, Zannone, and Palmarola) and the eastern group (Ventotene and Santo Stefano) (Figures 3 and 7).

The Ventotene basin infill shows here its maximum thickness of about 1.1–1.2 s (twt). The B unconformity is still affected by small extensional faults that do not propagate in the above sedimentary cover. A swell is onlapped by the lowermost part of the Plio-Pleistocene sequence, showing progressively more continuous reflectors. Symmetric folds, likely to be related to strike-slip positive structures, deform the Plio-Pleistocene sedimentary cover (Figure 7a); southwestward, the Plio-Quaternary sequence onlaps the structural high which delimited the Ventotene basin seaward.

Moving toward the SW, the seismic profile crosses the escarpment between the western and the eastern Pontine Archipelago. With respect to the northern TIR10-14, here the escarpment displays a more segmented structure, composed by more spaced NW-SE normal faults, which progressively lower toward the Vavilov plain the main unconformity B. In the upper part of the escarpment, mass flow deposits are characterized by a mounded geometry, transparent seismic facies at the bottom, and strong and continuous reflectors at the top, probably due to coarser sediments; it could be correlated with submarine mass wasting from the adjacent structural high. At Shot 950 a basement depression bordered by a fault plane shows an infilling

organized in a syncline geometry, likely due to gravity flow event originating from the margin to the NE; alternatively, the geometry showed by the reflectors could be linked to strike-slip movements (Figure 7b).

Further along the line, a rotated faulted block, 6–7 km long is imaged; it shows asymmetric flanks and is covered by a thin sedimentary succession, characterized by closely spaced reflections, with low to poor amplitude, slightly continuous and low acoustic impedance contrast, resulting somewhere in a transparent facies, suggesting a fine-grained nature of these sediment. It can be interpreted as a rotated block of the substratum, even if a volcanic nature can also be possible.

Further toward the Vavilov basin, the sedimentary cover is progressively thinner and it lies upon minor tilted blocks, formed by synthetic and antithetic faults. In addition at the end of the line a fault dipping toward the Vavilov basin cuts the seafloor, testifying recent or active tectonic activity here (Figure 7c).

5.3. TIR10-18 Seismic Profile

The TIR10-18 profile crosses the Ventotene basin between Ventotene and Ischia Islands (Figures 3 and 8). This line is shorter than the previous ones, and it does not reach the Vavilov basin, so it does not investigate the whole escarpment. The basin substratum is dissected by several extensional faults, probably linked to the NE-SW system affecting this part toward the Ischia Island. The basin infill, formed by parallel and continuous reflectors, reaches a maximum thickness of 0.7 s (twt), and progressively thins southwestward to the Ventotene volcanic complex (Shots 625–730). In this area some incipient faults cut the Plio-Quaternary sequence, with a very small offset (Figure 8a).

TIR10-18 crosses the escarpment south of Ventotene Island, where it extends over a wider area of about 70 km (in contrast with about 20 km in Ponza area to the north). In this way, the down-stepping toward the Vavilov basin results in a very gentle morphology, controlled by widely spaced listric normal fault, testifying a less localized deformation. A thin succession (no more than 0.2 s (twt)) overlies the substratum, and generally, no fault scarps are exposed, showing dominant depositional processes, thus contrasting with the northern region characterized by erosive processes (Figure 8b). At the bottom of the escarpment, a faulted basin is displayed, filled with almost 1 s (twt) of sediments; reflectors are mostly continuous and subparallel, onlapping toward the SW the rising basement (Figure 8c).

5.4. TIR10-13 Seismic Profile

TIR10-13 is the longest seismic profile of the data set; NW-SE trending, with a total length of about 200 km, it starts offshore Circeo Promontory and reaches the Salerno Gulf. For the aim of this study, the line was processed and interpreted in its northern 80 km: it starts at the edge of the continental margin immediately north of Palmarola basin, crosses the morphological high formed by the Ponza-Zannone alignment and then the central part of Ventotene basin, until the proximity with the Banco di Fuori and Ischia structural highs [*Aiello et al*., 2011] (Figures 3 and 9).

The continental margin offshore Circeo Promontory is characterized by a poor seismic resolution; due to the shallow water environment, strong sea bottom multiple reflections affected the acquisition and were difficult to eliminate during the processing. In particular, between shot points 5000 and 4700 in the proximity of the Zannone Island, seismic penetration is poor and seismic reflections are almost indistinguishable; this may be due to the main lithologies present in the area, composed by Meso-Cenozoic limestones exposed on the Zannone Island.

At Shot 4740 a NE-SW trending normal fault, dipping southeastward, divides the Ponza-Palmarola high from Ventotene basin (Figure 9). The sedimentary infill of the half graben is composed by different sequences delimited by several major unconformities, laterally thinning and onlapping the basal acoustic basement. This graben is divided in two depocenters by a cone-shaped structure (Figure 9a), whose origin seems to be volcanic [*Conti*, 2014; *Cuffaro et al*., 2016]. More to the SE, the line also crosses the lower part of the same Ventotene volcanic complex (Figure 9b).

5.5. TIR10-15 Seismic Profile

Line TIR10-15 has a WNW-ESE trend and crosses the abyssal plain of the Vavilov basin and in its portion in front of the western Pontine Islands area (Figures 3 and 10).

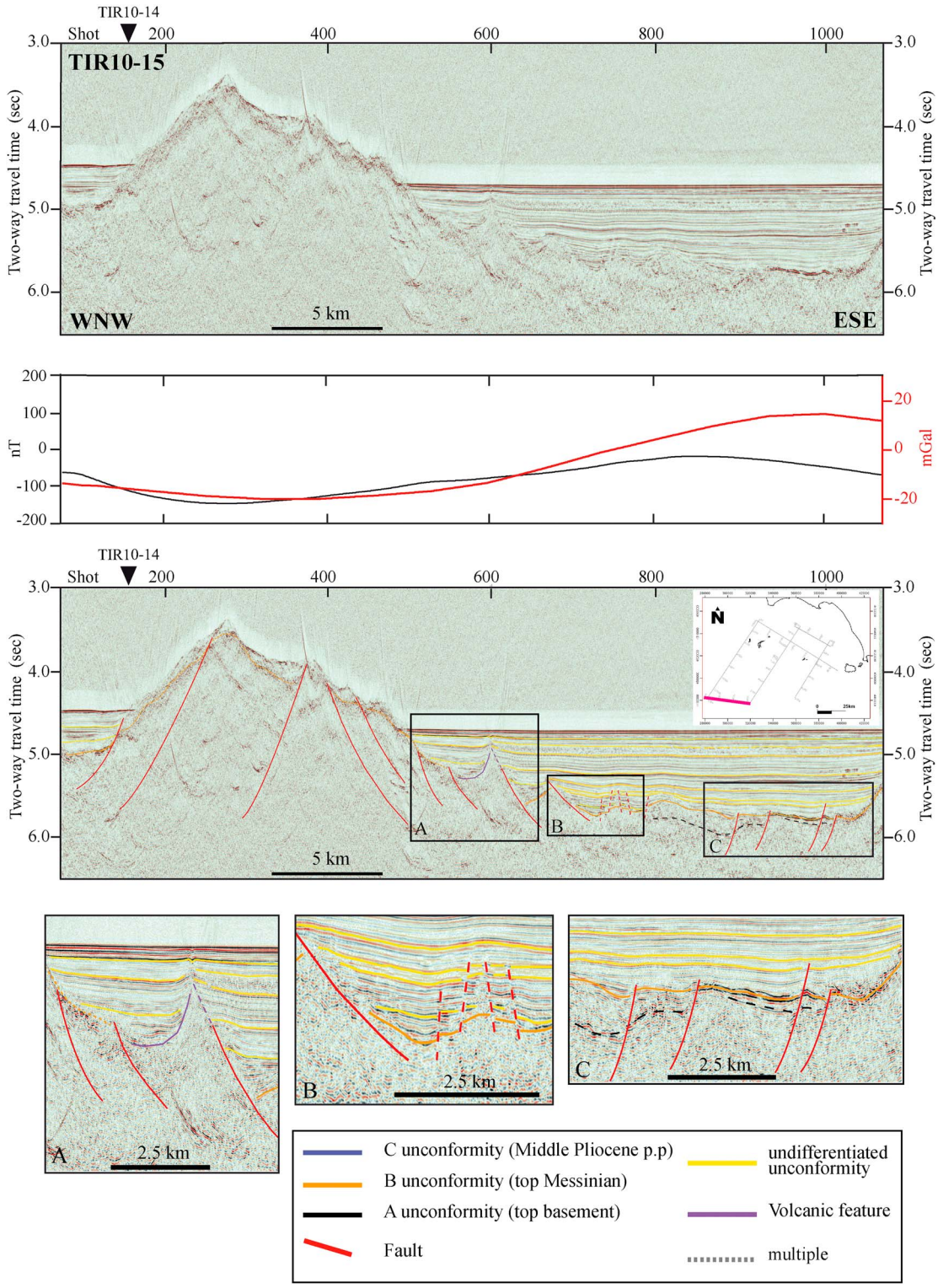

Figure 10. Kirchhoff time migrated seismic line TIR10-15, WNW-ESE directed, crossing the northern apex of the Vavilov abyssal plain (location shown in the white box). (top) Processed data only, with magnetic data (this study) and satellite-derived free air gravity anomaly from *Sandwell and Smith* [1997]. (bottom) Interpreted processed data; symbols provided by the legend. Insets: (a)Detail of a cone-like structure east of the Farfalla Smt.; the eastern flank is interested by a listric normal fault, with growth strata displayed at the hanging wall. This feature might represent a volcanic structure or a fluid/gas escape related feature. (b) Detail of the sedimentary infill of the Vavilov basin; the high angle faults with small offset interpreted could represent preferential paths for fluid escaping, as testified by the interruption of the seismic signal visible in this area. (c) The sedimentary fill of the Vavilov basin is composed by distal turbidites characterized by mostly continuous and parallel reflections; several faults dissect the substratum, which is probably composed by lava flows in the upper interval and serpentinized peridotites in the lower part.

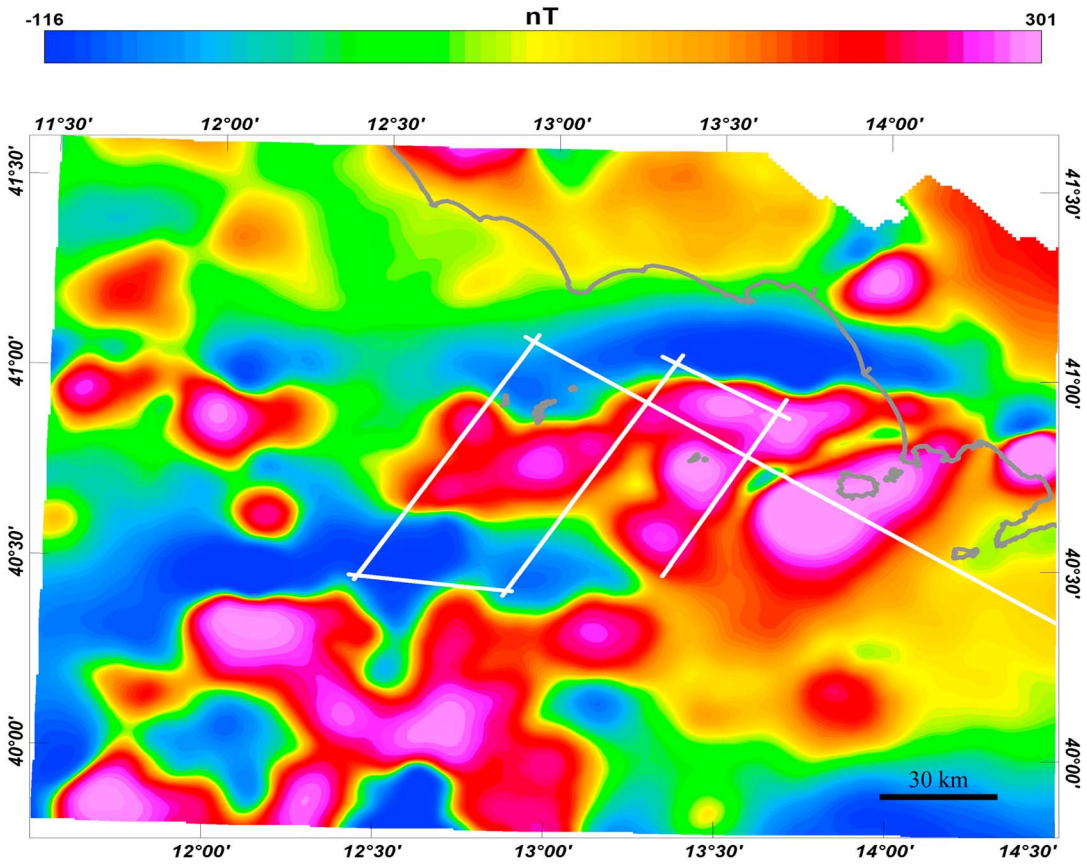

Figure 11. Magnetic anomaly of the Aeromagnetic map of Italy [*Caratori Tontini et al.*, 2004]. The studied area discussed in this work is marked by the white lines, representing the tracks of magnetic surveys of the Figure 2. See text for explanation.

Starting from the west, the seismic line crosses the Farfalla nonvolcanic seamount, which constitutes the western border of the Vavilov basin; this is one of the numerous seamounts present in the central Tyrrhenian basin. It has an asymmetric shape, with the western flank steeper than the eastern one; they are faulted by NNE-SSW trending normal faults. This rotated block is covered by a thin sedimentary cover, reaching about 0.1 s (twt). Immediately to the east of the Farfalla Smt., a cone-like structure is visible that might represent a volcanic feature; in alternatively, it could be related to a fluid/gas escape feature as chimneys penetrating vertically across the stratification and terminating at the seafloor. Fluid vents located near seamounts in the Tyrrhenian Sea have been previously highlighted [*Ligi et al.*, 2014; *Loreto et al.*, 2015]. At the eastern part of this feature a listric normal fault is imaged, with growth strata at the hanging wall (Figure 10a).

The Vavilov basin is imaged further along the line. It is formed by a sedimentary infill with a maximum thickness of 1.2 s (twt), thinner toward the east, near the basin margin; it shows mostly continuous and parallel reflections, with variable amplitude. Several faults seem to dissect the substratum and the bottom part of the sedimentary cover, probably composed by distal turbidites [*Gamberi and Marani*, 2004]. They are high angle faults with small offset that could represent preferential paths for fluid escaping, as testified by the anomaly of the seismic signal visible between Shots 750–780 that could be ascribe to this phenomenon (Figure 10b). The basement beneath the sedimentary units is composed by an upper set of reflectors, locally very bright (between shot points 996 and 1050), and a lower one, characterized by discontinuous reflectors displaying no clear dipping attitude (Figure 10c). Taking into account the drilling data of the ODP site 651, located about 35 km south of TIR10-15 line, the upper unit may correspond to the lava flows interval and the lower one to the basement made up of serpentinized peridotites (Figure 4). The seismic section ends to the east where the eastern escarpment bordering the Vavilov basin is intersected: this seems to be part of a major extensional fault system with an almost N-S direction, running from the Flavio Gioia high located to the south, until the base of the NW-SE escarpment bordering the margin offshore Ponza Island.

6. Magnetic Data

The five profiles cross a relative high magnetic anomaly area, as visible in the regional scale deduced from the Aeromagnetic Anomaly Map of Italy (Figure 11) [*Caratori Tontini et al.*, 2004]. In this map, the main volcanic structures of the Pontine Islands clearly match positive magnetic anomalies. The five magnetic anomaly profiles range from about −200 nT to about 400 nT.

In general, the profiles show magnetic anomaly patterns compatible with the occurrence of volcanic features, as highlighted in the interpreted seismic lines. The magnetized sources produce high-frequency relative maxima ranging from tens of nanotesla to up 400 nT.

In the central part of the line TIR10-13, for example, corresponding to the box B of Figure 9, a sequence of relative magnetic highs is clearly visible, with the highest at about 400 nT centered on the shot number 4025.

In the TIR10-14 the bathymetric high (centered on the shot number 800) corresponds to a relative high magnetic anomaly of about 85 nT, while the portion filled by sedimentary unit produce the decay of the magnetic anomaly value with apparent relative minimum (i.e., box A of Figure 6).

In the TIR10-15 line (Figure 10), the pronounced bathymetric structure of the Farfalla seamount produces a relative magnetic minimum of about −200 nT. *Prada et al.* [2014] found unexpected high seismic velocities for the Farfalla seamount and suggest the presence of mafic rocks. In this context, the negative value of the magnetic anomaly related to the Farfalla seamount could confirm the presence of mafic rocks older than the last normal chron (anomaly C1n, 780 ka).

7. Discussion

7.1. The Pontine Escarpment in the Geodynamic Context of the Central-Eastern Tyrrhenian Sea

The multichannel seismic profiles presented in this study provide new insights on the structural and geological framework of the Latium-Campania passive margin, and in particular on the geometry and structure of the escarpment connecting the deep Vavilov basin to the Italian shelf, which represents the dominant morphological feature of the surveyed area (Figure 12).

The Pontine escarpment represents the northern prolongation of a complex slope bordering the Vavilov abyssal plain. This main morphological feature bordering the Italian continental shelf is constantly narrowing from the Palinuro portion, where it reaches a width of 150 km, northward to the Pontine area, where it displays about 20 km of width [*Gamberi and Marani*, 2004]. It is characterized by three main dextral en echelon segments trending NW-SE and dipping to the SW: the northernmost Pontine escarpment, the Tacito escarpment, and the Palinuro seamount-Poseidon ridge; furthermore, another important feature characterizing this margin is the Sartori escarpment, immediately to the Northeast of the Tacito escarpment, constituted by three NNW-SSE segments (Figure 2). Tectonic activity strongly influenced the morphology and the depositional framework along this margin, together with other factors such as volcanic activity, distance from the mainland (low sedimentation rates) and bottom currents [*Conti et al.*, 2013].

Regional aeromagnetic anomaly map of the Tyrrhenian Sea [*Caratori Tontini et al.*, 2004] suggests that the Pontine area lies within an E-W elongated positive magnetic anomaly formed by coalescing of several large magnetic maxima related to volcanic structures of Ventotene and Ischia superimposed on a common low-frequency contribution. This suggests the presence of a deep common volcanic root connecting the Pontine and Ischia margins [*Cocchi*, 2007].

The E-W magnetic pattern of Pontine area is clearly bounded at south (Figure 11) where we observe a complex distribution of magnetic anomalies in the Vavilov basin due to the interference of signals from volcanic seamounts and those from extensional features [*Cocchi et al.*, 2008].

TIR-10 seismic survey highlighted progressive changes from north to south in the Pontine escarpment morphology, with a slope varying from steep to gentle and with an increasing number of extensional faults that constitute it. In the northern part, offshore the western Pontine archipelago, a single slope formed by few closely spaced extensional faults is responsible for the deepening of the margin, as well imaged on the seismic profile TIR10-14 (Figure 6). Here the escarpment is narrow, about 15 km, and it develops from 0.2 section to 4 s (twt), so it displays a high gradient. Moving to the south, the morphological feature is less obvious and the transition from the continental domain to the Vavilov basin occurs through several normal faults that offset

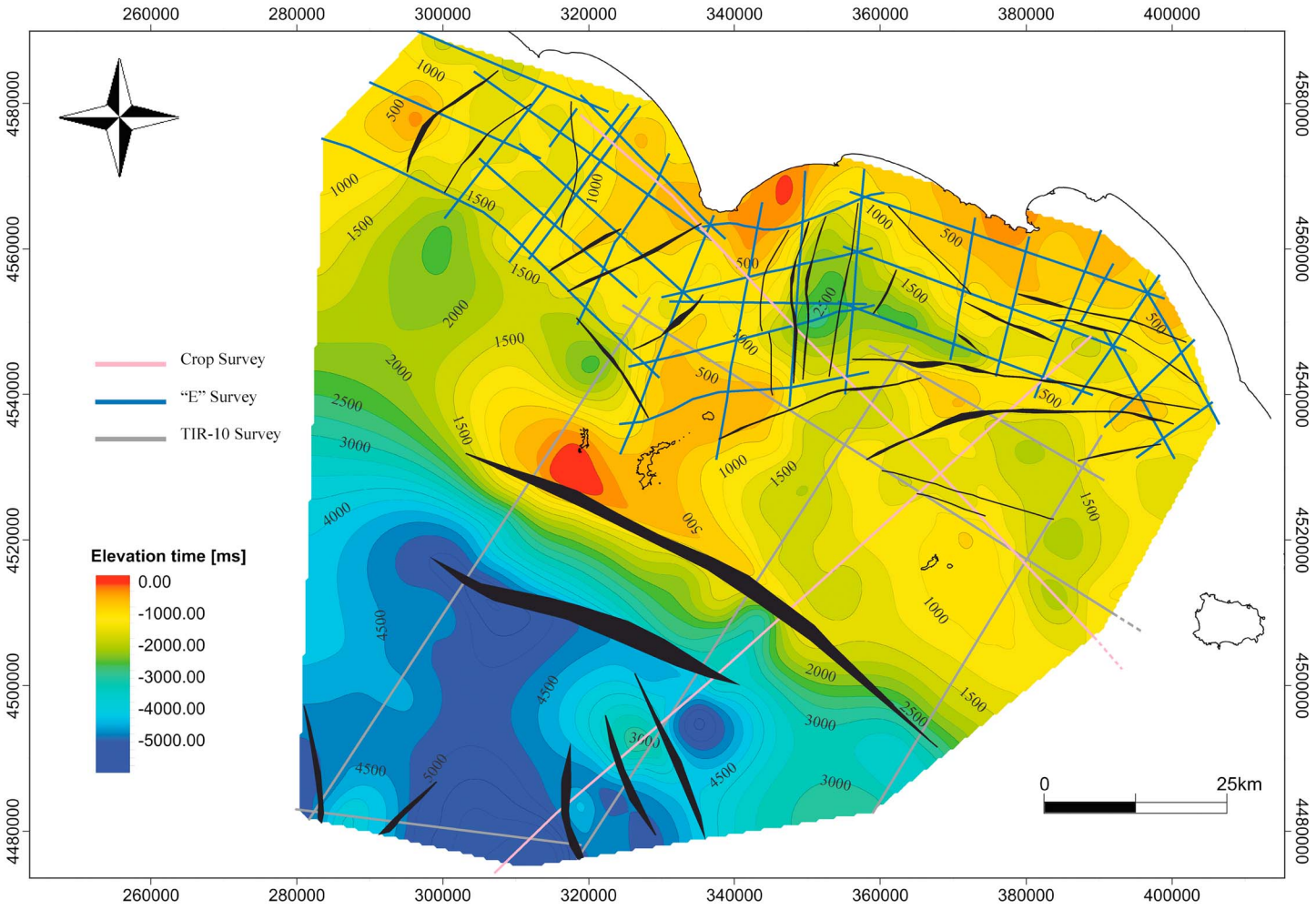

Figure 12. Contour map (TWT, ms) of the main basal unconformity (Top Messinian, orange horizon), showing main structural trends (NW-SE, NNW-SSE, and SW-NE) interpreted and correlated along the entire data set. The structural trend related to the escarpment is clearly shown and well constrained; minor faults interpreted are not represented because correlation among seismic lines is not possible.

progressively the top of the substratum, as observed in the line TIR10-18 (Figure 8). The spatial variation in the escarpment morphology corresponds to the progressive widening of the Vavilov basin itself toward the south. It accommodates the space available between the N-S structures that characterizes the deeper basin, as well as the Sardinian margin to the west, and the NW-SE structures that characterizes the Latium–Campania margin of the Tyrrhenian Sea to the east.

In our interpretation this escarpment is the main feature of the area, controlled by the strong extensional phase related to the Tyrrhenian basin opening that took place at the beginning of Early Pliocene. This tectonic lineament is probably still active, as testified by the huge instability processes observed, by the lack or the minimum amount of sediment accumulation on the structural high portions or by the growth fault structure displayed by some reflectors. This conclusion is supported also by the instrumental and historical seismicity analysis provided by *Favali et al.* [2004], which highlight seismicity (although of low values, in both occurrence and energy) in the offshore area of the Pontine islands. The escarpment corresponds to a strong localization of the deformation in the north, where the morphology is steep and formed by only one fault plane. In the south the deformation is more distributed along several faults, and the escarpment shows a gentler slope. Even the strike is different, the northern segment of the escarpment has an NW-SE trend, whereas southward, on seismic lines TIR10-16 and TIR10-18, faults has a NNW-SSE trend, which is responsible for the setting of the margin itself. This latter trend slightly follows the direction of the Sartori Escarpment [*Curzi et al.*, 2003].

On a basin scale, deformation starts in the proximity of the retreating slab, with faults striking parallel (NW-SE) to the arc, whereas they become progressively oblique to the arc in later stages. This is in agreement with the results obtained by *Schellart et al*. [2003], using analogue models to simulate asymmetric deformation of an overriding plate due to anticlockwise rollback of a subducting plate. Moreover, as highlighted by the differences described between TIR10-14 and TIR10-18, extension along the margin is accommodated by increasing deformation toward the far end of the retreating boundary, whereas it is localized on a narrow fault zone toward the north; this is also observed in others wedge-shaped back-arc basins, as the Kuril Basin [*Schellart et al*., 2003], the North Fiji back-arc Basin bordering the New Hebrides arc [*Schellart et al*., 2002], or the Lau back-arc Basin bordering the Tonga arc [*Bevis et al*., 1995]. Even in the Tyrrhenian sea, the relationship between slab retreat and back-arc extension generates the coexistence of different trends: NW-SE, NNW-SSE, and N-S; at the same time, this implies the occurrence of different kinematics along the faults planes, as results from the presented seismic interpretation, which indicates the occurrence of high angle faults, associated to anticlines or to small flower structures) compatible with a strike-slip kinematic, even if the general setting is largely dominated by extensional normal faults (Figure 7, A and B boxes).

In this context, the NNW-SSE trending lineament system that constitutes the southern part of the Pontine escarpment, as described in this work, represents a transfer zone, characterized by a dextral strike-slip component and is composed by normal faults organized in an en echelon left-lateral geometry. This transtensional system accommodates the increasing extension through a redistribution of the deformation within the NW-SE dextral transfer fault system (from the Pontine Escarpment to the Palinuro seamount-Poseidon ridge) (Figure 3). From a geodynamic viewpoint, the apparent left-lateral offset along the NW striking faults may be ascribed to the left-lateral transpression related to the eastward migration of the Apennines compressive front [*Doglioni*, 1991; *Doglioni et al*., 1999].

Transverse systems, with oblique strike respect to the main set of extensional faults, can occur in extensional settings; in many cases, they are interpreted as tear faults of the normal faults, for example, in the North Sea [*Gibbs*, 1984], the Suez Rift [*McClay and Khalil*, 1998], and the Atlantic margin of Norway [*Dore' et al*., 1997; *Tsikalas et al*., 2001]. In particular, *Acocella and Funiciello* [2006] pointed out the presence, along the Tyrrhenian margin of central Italy, of NW-SE normal faults related to back-arc extension, together with coeval NE-SW transverse system, characterized by a dominant strike-slip kinematic. Analogue models performed by the same authors have determined that for relative lower stretching factor ($\beta < 1.3$) interaction between nearby extensional structures occurs through the formation of relay ramps; in contrast, for $\beta > 1.3$, transfer faults develop, subparallel to the extension direction. The transition between areas with high- and low-extension rates is characterized by structures striking oblique to the main direction of extension, with a strike-slip component. This latter situation could be applied to our study area, where the NW-SE transfer faults area associated with the N-S coeval normal faults.

The described structural setting is consistent with a stepwise eastward migration of the contractional active front and with the southeastward Calabrian slab rollback, which generates extension in the back-arc area [*Doglioni*, 1991]. This latter, started after the early Pliocene, is responsible for the migration of the main volcanic activity from the Vavilov to the Marsili and, at the same time, of the E-W extensional regime within the Tyrrhenian Sea. This migration can also be connected to different rate of deformation in the Southern Tyrrhenian Sea with respect to the northern portion of the basin [*Patacca et al*., 1990; *Doglioni*, 1991; *Faccenna et al*., 1997; *Carminati et al*., 2010].

It is worth to notice that in contrast to what observed along the Apennine chain, in the Vavilov abyssal plain the E-W direction of extension persists, and the basin is controlled by a N-S trending group of extensional faults [*Sartori et al*., 2004].

Merging and comparing our results with those from adjacent regions [*Turco et al*., 2010; *Milia and Torrente*, 2015; *Milia et al*., 2016b] allow us to attempt a sketch of the tectonic evolution of the central-eastern Tyrrhenian margin.

Plate tectonic framework is investigated with kinematic reconstructions based on work of *Carminati et al*. [2010] with respect to fixed Eurasia. Figure 13, panels from 7 Ma to 0 Ma, show the chronological migration of Apennines thrust front and the Calabria, the growth of the Apennines Belt, and the opening of the Tyrrhenian Sea (back-arc stretched area).

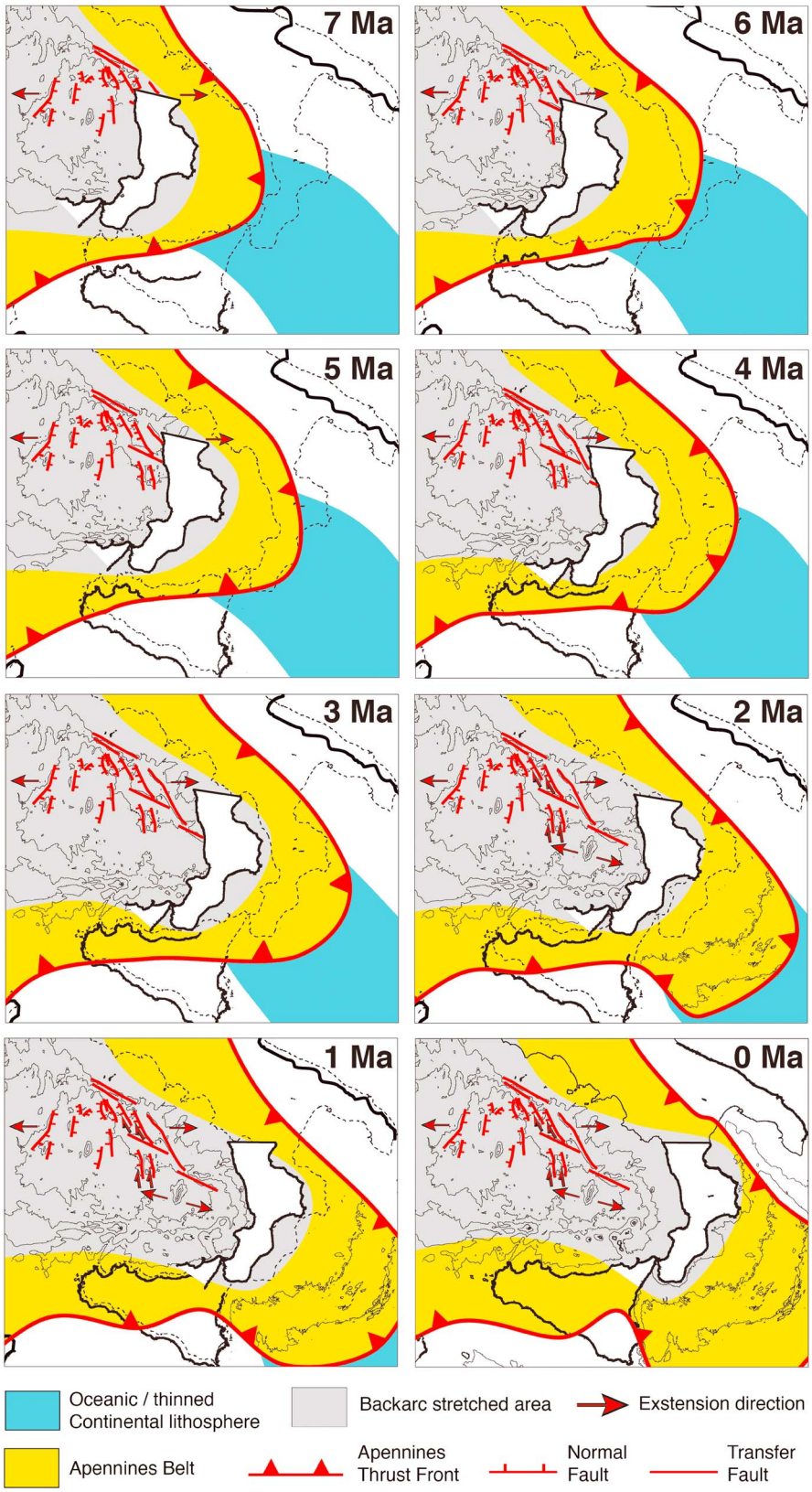

Figure 13. Tectonic and kinematic evolution from 7 to 0 Ma in the central and southern Tyrrhenian Sea with respect to fixed Eurasia. The dashed line is the present-day position of the italian coastlines. Data from *Carminati et al.* [2010]. See text for explanation.

Since 7 Ma extension, generally E-W directed, caused the formation of the Vavilov basin and strongly affected the eastern Tyrrhenian margin, generating several NNW-SSE normal faults and few NW-SE transfer faults bounding the deepest part of the basin. Panels from 6 to 3 Ma show eastward migration of extension over a wide area, maintaining the same direction of extension and increasing the number of normal and transfer faults. On the Tyrrhenian margin this stage of rifting is characterized by almost N-S, NE-SW, and ENE-WNW trending faults (Figure 12), which caused grabens and half-grabens formation filled by clastic sediments during Plio-Quaternary times. Exhumation of mantle rocks and emplacement of basalts in the Vavilov area took place at this stage [*Milia et al*., 2013], and volcanic activity developed at Ponza (4.0–1.0 Ma).

At 2 Ma, strain localization stepped outside the initial rift system and moved toward SE into the Marsili basin area, with the beginning of the volcanic activity at Marsili Volcano. Also, the extension direction moved from E-W to NW-SE causing the opening of the Marsili basin, and resulting in an oblique deformation component on the previously formed normal faults. The Pontine escarpment and the southern segment of the escarpment (Tacito escarpment and Palinuro-Poseidon ridge) acted as transfer faults, accommodating the increasing amount of extension to the southeast.

During this stage, in the northern part of the study area (southern Latium region), fault activity along the marginal basins of the Latium-Campania margin gradually stopped; on the contrary, faults were still active in the southern area (Campania region) with a prevalence of NNE-SSW and E-W striking directions [*Conti*, 2014]. Volcanism is widespread in the Roman and Campania provinces [*Lustrino et al*., 2011].

Taking into account the framework outlined above, the tectonic extension affecting the eastern Tyrrhenian slope can be interpreted as an expression of the combination of different geodynamic movement, associated to the complex Tyrrhenian-Apennines system, which is controlled by a progressive retreat of the slab and the progressive migration to southeast, generating a extensional-right-lateral regime in the back-arc basin [*Doglioni*, 1991]. In this context also the different distribution of deformation could be considered as due to a progressive increment of combination between extension and oblique tectonics, required to transfer the extension throughout the eastern Tyrrhenian margin to southeast along a complex fault system composed by the Pontine escarpment, the Palinuro seamount-Poseidon ridge, and the Tacito escarpment [*Turco et al*., 2010].

The asymmetric retreat of the slab and the increasing deformation toward the far end of the slab accommodating the extension is characteristic of others wedge-shaped back-arc basins, such as the Kuril Basin or the North Fiji back-arc Basin [*Schellart et al*., 2002, 2003], as previously reported. Transfer zones (here represented by the Pontine escarpment and in the southern area by the Tacito escarpment and the Palinuro seamount-Poseidon ridge) are intended as zones of oblique or strike-slip faulting that transfer strain between spatially separated domains of extension. It is worth mentioning that, for example, *Moy and Imber* [2009] reported similar faults transferring extensional strain between en-echelon rift segments in the NE Atlantic margin.

7.2. Crustal Structure of the Tyrrhenian sea

Data from TIR-10 survey are not able to clearly unravel the deep crustal structure of the investigated area, fundamentally due to the acquisition parameters and the presence of strong water-layer multiples that mask the deeper reflections.

Nevertheless, integrating our results from the TIR-10 survey, with recent works investigating the nature of the Tyrrhenian crustal domains, such as those of *Prada et al*. [2015, 2016] and *Sartori et al*. [2004], we produced two representative geological sections in order to propose an updated interpretation of the crustal structure in the study area (Figure 14).

The eastern part of the NE-SW trending seismic lines TIR10-14, TIR10-16, and the entire TIR-18 crosses a region of continental crust progressively thickening toward the continent (about 15 km [*Prada et al*., 2015], which represents the westernmost extension of the eastern Tyrrhenian margin. *Prada et al*. [2015] report velocities in the order of 5.5–6.5 km/s, compatible with a continental domain; Moho reflections are not visible probably due to the multiple energy that masks the image. This domain presents a segmented basement morphology, cut by extensional faults not reaching the seafloor and showing little displacements (in the order of tens of milliseconds).

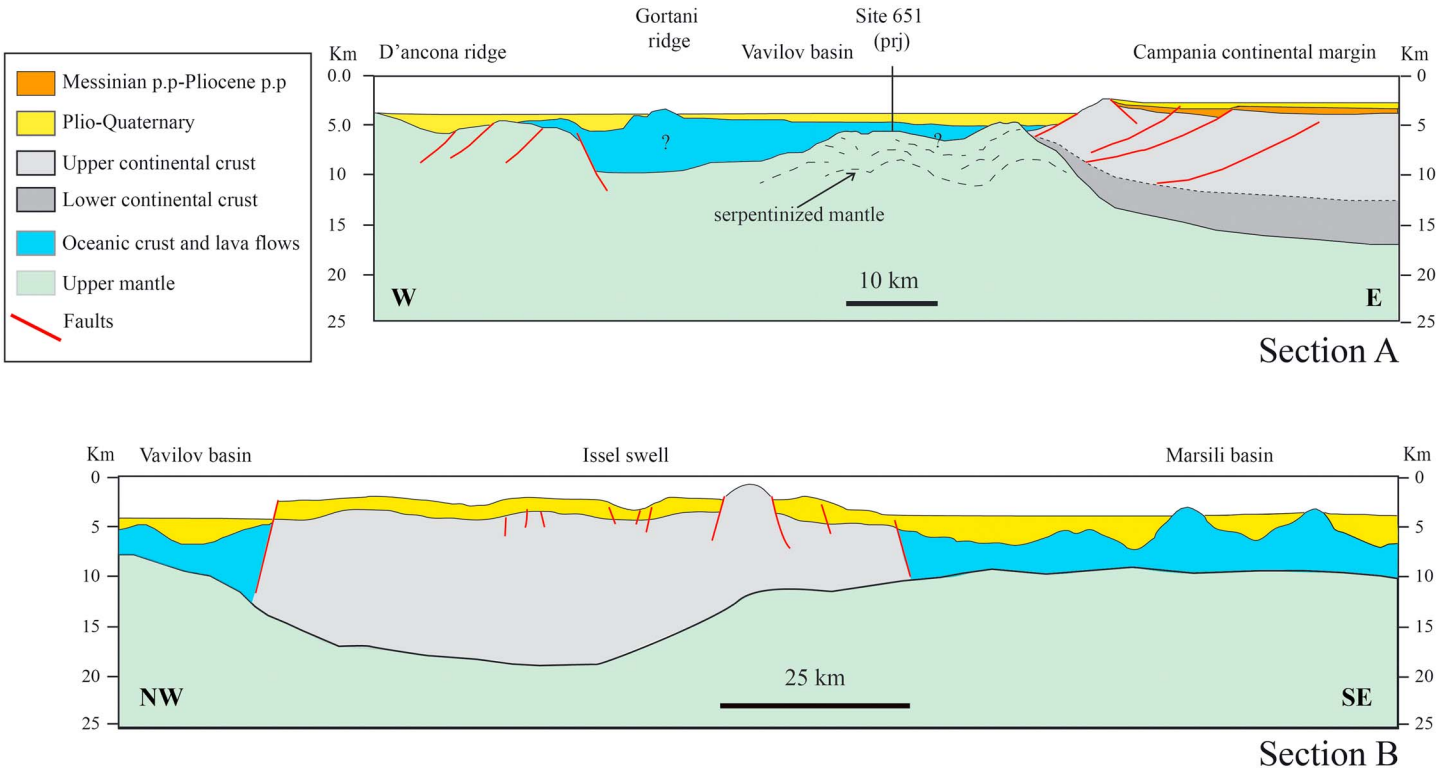

Figure 14. Crustal-scale geological sketches of the Tyrrhenian basin (a) across the Campania continental margin and the central area of Vavilov basin and (b) across the Vavilov basin, Issel swell, and Marsili basin. The two sections display the geometrical relationship between the different crustal domains characterizing the Tyrrhenian basin, i.e., continental crust, ultrathinned continental crust, exhumed mantle, and uncertain oceanic crust. Crosslines location in Figure 2 (Modified after *Sartori et al.* [2004] and *Doglioni et al.* [2004]).

Moving offshore, the TIR10-14 (from Shot 1300) and TIR10-16 (from SP 1000) cross a domain characterized by pervasive normal faults which cut through the seafloor, thus, strongly controlling its morphology (offsets are in the order of hundreds of ms); for instance, the tilted and faulted block of the Farfalla seamount (Figure 10), or the faulted block displayed on TIR10-16 (Figure 7, SP 600). According to *Prada et al.* [2015] these parts correspond to stretched and thinned continental crust (6–8 km). Extension in this region is accommodated mostly by normal faulting, such as in other magma-poor margins, where crustal thinning due to normal faults, with heaves of several km, yields large tilted fault-blocks [*Ranero and Pérez-Gussinye*, 2010]. In the southern area, the Tyrrhenian basin opening is mostly associated with magmatic accretion, resulting in a gentler topography and smaller offsets along the faults, as highlighted by *Prada et al.* [2015].

TIR10-15 crosses the northern tip of the Vavilov basin, filled with about 1.2 s (twt) thick sedimentary sequence and bordered by major faults on both sides of the basin (Figure 10). The basin infill is mostly horizontal and continuous, whereas basement shows the presence of several faults in the uppermost part. Stacking velocities obtained from the processing of the TIR-10 lines are actually higher in this area where high-amplitude and bright reflections are visible that can be tentatively ascribed to basalt flows. *Kastens and Mascle* [1990] and *Sartori et al.* [2004] assumed that the Vavilov abyssal plain is floored by oceanic crust; in contrast, data from *Prada et al.* [2015, 2016] support the presence of an exhumed mantle basement. In particular, *Prada et al.* [2016] indicate the presence of serpentinized mantle in the northern tip of the Vavilov basin in a 4–5 km-narrow region; a conclusion based on the absence of Moho reflections and by a *P* wave velocity gradient consistent with the vertical velocity structure of other exhumed mantle regions. The extensional faults bordering the basin are probably preferred pathways for fluids circulation causing serpentinization (Figure 10). These authors also suggest that the exhumed mantle in the Vavilov basin is locally intruded by MORB-like (for example the Gortani Ridge; Figure 3) and/or by intraplate basaltic melts (the Magnaghi and Vavilov volcanoes; Figure 3), emplaced at the same time or soon after the exhumation.

In the CROP-section M2A/b crossing the Marsili basin, scattered deep reflectors at a depth of ~6 km attributed to the Moho [*Doglioni et al*., 2004] suggest that the basin is floored by oceanic crust [*Kastens and Mascle*, 1990; *Marani and Trua*, 2002]. Inversion of high-resolution magnetic data from the Marsili region by *Cocchi et al*. [2009] reveals NNE-SSW magnetization stripes with the oldest dated at 1.77 Ma (late Matuyama), implying an average full spreading rate of ~28–31 mm/a; since 1.07 Ma, spreading rate decreased to 18 mm/a inducing a vertical growth of the Marsili volcanic edifice.

Mantle unroofing and exposure of upper mantle rocks is an important consequence of magma-poor rifting and/or seafloor spreading even in small back-arc basins such as the Tyrrhenian sea [*Lagabrielle*, 2009]. However, based on the considerations previously exposed, it is clear that the classic models proposed for magma-poor hyper-extended margins and mantle exhumation [*Pérez-Gussinyé et al*., 2003; *Lavier and Manatschal*, 2006], in which a spatial sequence of continental crust, mantle exhumation, and finally oceanic crust is expected, is not applicable for the Tyrrhenian sea. In fact, continent-ocean transition zone and continent-ocean boundary are not well defined in this basin, as it occurs instead for example in the Iberia-Newfoundland margins [*Whitmarsh and Wallace*, 2001] or in the South China Sea [*Franke et al*., 2014]. Also, the abundant magmatic activity accommodating the extension in the southern Tyrrhenian basin and the magmatic intrusions within the exhumed mantle are in contrast with the negligible volcanism occurred during crustal thinning and mantle exhumation in the Iberia and South China Sea margins, where continent-ocean transition zones do not expose volcanic products and where most of the magmatic activity took place after seafloor spreading initiation [*Franke et al*., 2014].

The Tyrrhenian basin presents differences also if compared to other back-arc basins of the Mediterranean region; for example, the Ligurian-Provencal basin opened with the formation of narrow, linear, and localized spreading centers [*Faccenna et al*., 1997]. In particular, in the Gulf of Lion, which is part of the Liguria-Provencal basin, transition to the oceanic domain occurs with exhumed lower crust and exhumed mantle [*Jolivet et al*., 2015], through a series of shallow-dipping detachments. In contrast, in the Tyrrhenian basin deformation and magmatism are spread over a wide area and extension migrated inside the basin [*Faccenna et al*., 1997]. A lower Pliocene detachment seems to be responsible for mantle exhumation in the Vavilov basin [*Kastens et al*., 1988; *Mascle and Rehault*, 1990; *Milia et al*., 2013], generally placed at a depth of about 10 km [*Prada et al*., 2016].

The structural complexity of the Tyrrhenian back-arc basin can be ascribed to several causes: extension of the Tyrrhenian Sea affected the Apenninic fold and thrust belt soon after the onset of the shortening, so inherited geologic features of the subducting slab could have promoted the weakening of the lithosphere [*Faccenna et al*., 1997]; the onset of oblique slip within the general extensional setting of the central-eastern Tyrrhenian margin highlighted by this study, which could have played an important role in preventing the formation of a large ocean-continent transition zone in the study area, and finally, the role played by the stretching velocity, that in back-arc regimes, depends upon the velocity of the sinking lithosphere [*Faccenna et al*., 1997].

8. Conclusions

A detailed stratigraphic and structural analysis of the central-eastern margin down to the abyssal plain of the Tyrrhenian Sea has been carried out based on the interpretation of new seismic reflection profiles acquired during cruise TIR-10 and constrained by data from wells logs and other seismic lines available in the area (CROP and ViDEPI data set).

Our data highlight the morphological variation of the Pontine escarpment from north to south, corresponding to a partitioning of deformation. A steeper margin to the north corresponds to a steeper fault scarp, as well as a smooth slope in the south corresponds to several more distributed normal faults. These latter are organized in an en echelon setting, and in our view they transfer the extension along the main escarpment, composed, at the basin scale, by the Pontine-Tacito-Palinuro fault system. In this framework, the occurrence of different normal fault trends throughout the eastern Tyrrhenian margin suggests the presence of different kinematics along the main fault planes; i.e., a generally oriented E-W extension induces a dextral strike-slip component on these faults.

Combining our data with other published results, we unravel the nature of crust in the study area, that is composed by continental crust intruded by back-arc related volcanism along the margin and by exhumed mantle peridotites with uncertain presence of oceanic crust in the central abyssal plain (Figure 14).

The kinematic evolution we propose (Figure 13) takes into account a leap in the locus of strain localization related to the opening of the Marsili basin, together with a change in rifting direction (NW-SE), implying an oblique component on the N-S lineaments accommodated by the transfer zone composed by the Pontine-Tacito-Poseidon escarpments.

This feature can be considered as the expression of the asymmetry of the basin due to the slab retreat mechanism from NW to SE and the consequent migration of contractional deformation and active volcanism [*Doglioni*, 1991; *Carminati et al*., 2010; *Bortoluzzi et al*., 2010]. The northern sector of the Pontine-Tacito-Palinuro fault system can be considered as the transition zone between two areas with a different amount of extension, lower in the north and higher in the south. This transition probably controls the escarpment geometry, determining the different morphology along the Pontine escarpment.

Classical rifting models can hardly explain the peculiarities observed in the opening and evolution of the Tyrrhenian basin; the complex structural setting of this basin can be ascribed both to inherited geologic features of the subducting slab and to the stretching velocity, related to the velocity of the sinking lithosphere. An important role in the evolution of the margin is also played by the onset of strike slip or oblique tectonics within the general extensional setting, as shown by this study (Figure 13). In fact, this may have prevented the formation of a large ocean-continent transition zone and may have reduced or inhibited oceanic crust production in the study area.

Recently, *Milia et al*. [2016a] infer the existence of a STEP fault (Subduction-Transform-Edge-Propagator) along the northern margin of the Ionian slab; the transfer fault zones highlighted in this study can be tentatively interpreted as an upper plate response to the STEP fault onset during rollback of the Ionian slab.

Acknowledgments

The officers and the crew of the R/V *Urania*, owned and operated by SO.PRO. MAR., and the scientific party of the TIR-10 survey are thanked for their cooperation during fieldwork. This research was supported by the Consiglio Nazionale delle Ricerche (CNR) of Italy under the sponsorship of The Dipartimento Terra Ambiente and his formed Director Giuseppe Cavaretta. Author greatly thank Schlumberger Company for providing an educational license of Petrel software, used for seismic interpretation and interpolations. Authors greatly appreciate the suggestions given by the Associated Editor and the reviewers A. Billi and Y. Lagabrielle, which significantly helped in the improvement of the paper. Original multichannel seismic data are available upon request at the CROP database (www.crop.cnr.it); magnetic data related to TIR-10 survey are available upon request.

References

Acocella, V., and F. Rossetti (2002), The role of extensional structures on pluton ascent and emplacement: The case of southern Tuscany (Italy), *Tectonophysics*, *354*, 71–83, doi:10.1016/S0040-1951(02)00290-1.

Acocella, V., and R. Funiciello (2006), Transverse systems along the extensional Tyrrhenian margin of central Italy and their influence on volcanism, *Tectonics*, *25*, TC2003, doi:10.1029/2005TC001845.

Aiello, G., E. Marsella, A. G. Cicchella, and V. Di Fiore (2011), New insights on morpho-structures and seismic stratigraphy along the Campanian continental margin (Southern Italy) based on deep multichannel seismic profiles, *Rend. Fis. Acc. Lincei*, *22*, 349–373.

Barberi, F., S. Borsi, G. Ferrara, and F. Innocenti (1967), Contributo alla conoscenza vulcanologica e magmatologica delle Isole dell'Archipelago Pontino, *Mem. Soc. Geol. Ital.*, *6*, 581–606.

Barbieri, M., P. Di Girolamo, E. Locardi, G. Lombardi, and D. Stanzione (1979), Petrology of the calc-alkaline volcanics of the Parete 2 well (Campania, Italy), *Per. Mineral.*, *48*, 53–74.

Bartole, R. (1984), Tectonic structures of the Latian-Campanian shelf (Tyrrhenian Sea), *Boll. Ocean. Teoritica. Appl.*, *2*, 197–230.

Bartole, R. (1990), Caratteri sismostratigrafici, strutturali e paleogeografici della piattaforma continentale tosco-laziale; suoi rapporti con l'Appennino settentrionale, *Boll. Soc. Geol. Ital.*, *109*, 599–622.

Beccaluva, L., et al. (1990), Geochemistry and mineralogy of volcanic rocks from the ODP Sites 650, 651, 655 and 654 in the Tyrrhenian Sea, in *Proceedings of the Ocean Drilling Program, Scientific Results*, vol. 107, edited by K. A. Kastens et al., pp. 49–74, Ocean Drilling Program, College Station, Tex.

Bellotti, P., P. Evangelista, P. A. Tortora, and P. Valeri (1997), Caratteri sedimentologici e stratigrafici dei sedimenti Plio-Pleistocenici affioranti lungo la costa tra Tor Caldara e Anzio (Lazio centrale), *Boll. Soc. Geol. Ital.*, *116*, 79–94.

Bellucci, F., M. Grimaldi, L. Lirer, and A. Rapolla (1997), Structure and geological evolution of the island of Ponza, Italy: inferences from geological and gravimetric data, *J. Volcanol. Geother. Res.*, *79*, 87–96.

Bevis, M., F. W. Taylor, B. E. Schutz, and S. Calmant (1995), Geodetic observations of very rapid convergence and backarc extension at the Tonga arc, *Nature*, *374*, 249–251.

Billi, A., V. Bosi, and A. De Meo (1997), Caratterizzazione strutturale del rilievo del Monte Massico nell'ambito dell'evoluzione quaternaria delle depressioni costiere dei fiumi Garigliano e Volturno (Campania settentrionale): Il Quaternario, *Ital. J. Quat. Sci.*, *10*, 15–26.

Bortoluzzi, G., et al. (2010), Interactions between volcanism and tectonics in the western aeolian aector, Southern Tyrrhenian Sea, *Geophys. J. Int.*, *183*, 64–78.

Brogi, A., E. Capezzuoli, I. Martini, M. Picozzi, and F. Sandrelli (2014), Late Quaternary tectonics in the inner Northern Apennines (Siena Basin, southern Tuscany, Italy) and their seismotectonic implication, *J. Geodyn.*, *76*, 25–45, doi:10.1016/j.jog.2014.03.001.

Bruno, P. P., V. Di Fiore, and G. Ventura (2000), Seismic study of the '41st Parallel' Fault System offshore the Campanian–Latial continental margin, Italy, *Tectonophysics*, *324*, 37–55.

Buttinelli, M., D. Scrocca, D. De Rita, and F. Quattrocchi (2014), Modes of stepwise eastward migration of the northern Tyrrhenian Sea back-arc extension: Evidences from the northern Latium offshore (Italy), *Tectonics*, *33*, 187–206, doi:10.1002/2013TC003365.

Cadoux, A., D. L. Pinti, C. Aznar, S. Chiesa, and P. Gillot (2005), New chronological and geochemical constraints on the genesis and geological evolution of Ponza and Palmarola volcanic islands (Tyrrhenian Sea, Italy), *Lithos*, *81*, 121–151.

Caratori Tontini, F., P. Stefanelli, I. Giori, O. Faggioni, and C. Carmisciano (2004), The revised aeromagnetic anomaly map of Italy, *Ann. Geophys.*, *47*, 1547–1555.

Caratori Tontini, F., F. Graziano, L. Cocchi, C. Carmisciano, and P. Stefanelli (2007), Determining the optimal Bouguer density for a gravity data set: Implications for the isostatic setting of the Mediterranean Sea, *Geophys. J. Int.*, *169*, 380–388.

Caratori Tontini, F., L. Cocchi, and C. Carmisciano (2008), Potential-field inversion for a layer with uneven thickness: The Tyrrhenian Sea density model, *Phys. Earth Planet. Inter.*, *166*, 105–111, doi:10.1016/j.pepi.2007.10.007.

Carminati, E., and C. Doglioni (2012), Alps vs. Apennines: The paradigm of a tectonically asymmetric Earth, *Earth Sci. Rev.*, *112*, 67–96, doi:10.1016/j.earscirev.2012.02.004.

Carminati, E., M. J. R. Wortel, W. Spakman, and R. Sabadini (1998), The role of slab detachment processes in the opening of the western-central Mediterranean basins: some geological and geophysical evidence, *Earth Planet. Sci. Lett*, *160*, 651–665.

Carminati, E., M. Lustrino, M. Cuffaro, and C. Doglioni (2010), Tectonics, magmatism and geodynamics of Italy: What we know and what we imagine, *J. Virtual Explor.*, *36*, 9.

Carminati, E., M. Lustrino, and C. Doglioni (2012), Geodynamic evolution of the central and western Mediterranean: Tectonics vs. igneous petrology constraints, *Tectonophysics*, *579*, 173–192.

Cavinato, G. P., D. Cosentino, D. De Rita, R. Funiciello, and M. Parotto (1994), Tectonic-sedimentary evolution of intrapenninic basins and correlation with the volcano-tectonic activity in central Italy, *Mem. Descr. Carta Geol. Ital.*, *49*, 63–76.

Cella, F., M. Fedi, G. Florio, V. Paoletti, and A. Rapolla (2008), A review of the gravity and magnetic studies in the Tyrrhenian basin and its volcanic districts, *Ann. Geophys.*, *51*(1), doi:10.4401/ag-3035.

Chiocci, F. L., and L. Orlando (1996), Lowstand terraces on Tyrrhenian Sea steep continental scope, *Mar. Geol.*, *134*, 127–143.

Chiocci, F. L., E. Martorelli, and A. Bosman (2003), Cannibalization of a continental margin by regional scale mass wasting: an example from the central Tyrrhenian Sea, in *Submarine Mass Movements and Their Consequences*, edited by J. Locat and J. Mienert, pp. 409–416, Kluwer Acad., Dordrecht, Netherlands.

Civetta, L., G. Orsi, P. Scandone, and R. Pece (1978), Eastwards migration of the Tuscan anatectic magmatism due to anticlockwise rotation of the Apennines, *Nature*, *276*, 604–606.

Cocchi, L. (2007), Magnetic structural evidences of the 41st parallel zone (Tyrrhenian Sea) inferred from potential field data: the 3D model of the discontinuity, PhD thesis, University of Bologna.

Cocchi, L., F. Caratori Tontini, C. Carmisciano, and M. Marani (2008), Tortonian-Pleistocenic oceanic features in the Southern Tyrrhenian Sea: Magnetic inverse model of the Selli-Vavilov region, *Mar. Geophys. Res.*, *29*(4), 251–266, doi:10.1007/s11001-009-9061-5.

Cocchi, L., F. Caratori Tontini, F. Muccini, M. P. Marani, G. Bortoluzzi, and C. Carmisciano (2009), Chronology of the transition from a spreading ridge to an accretional seamount in the Marsili backarc basin (Tyrrhenian Sea), *Terra Nova*, *21*, 369–374, doi:10.1111/j.1365-3121.2009.00891.x.

Conti, A. (2014), Processing and interpretation of new multichannel seismic profiles. The Central Eastern margin of the Tyrrhenian basin, PhD thesis, Sapienza Università di Roma, Rome, Italy.

Conti, M. A., D. E. Girasoli, V. Frezza, A. M. Conte, E. Martorelli, R. Matteucci, and F. L. Chiocci (2013), Repeated events of hardground formation and colonization by endo-epilithozoans on the sediment-starved Pontine continental slope (Tyrrhenian Sea, Italy), *Mar. Geol.*, *336*, 184–187.

Cornamusini, G., A. Lazzarotto, S. Merlini, and V. Pascucci (2002), Eocene-Miocene evolution of the north Tyrrhenian Sea, *Boll. Soc. Geol. Ital.*, *Spec.1*, 769–787.

Cuffaro, M., et al. (2016), The Ventotene Volcanic Ridge: A newly explored complex in the central Tyrrhenian Sea (Italy), *Bull. Volcanol.*, *78*, 86, doi:10.1007/s00445-016-1081-9.

Curzi, P. V., A. Castellarin, G. B. Vai, and N. Zitellini (2003), Raimondo Selli e Renzo Sartori una staffetta generazionale della geologia marina italiana. In: Convegno in memoria di Raimondo Selli e Renzo Sartori. La geologia del Mar Tirreno e degli Appennini. Bologna, 1-12 December 2003.

D'argenio, B., T. S. Pescatore, and P. Scandone (1973), Schema geologico dell'Appennino meridionale (Campania e Lucania), *Atti Accad. Naz. Lincei Quad.*, *183*, 49–72.

De Rita, D., R. Funiciello, D. Pantosti, F. Salvini, A. Sposato, and M. Velona (1986), Geological and structural characteristics of the Pontine islands (Italy) and implications with the evolution of the Tyrrhenian margin, *Mem. Soc. Geol. Ital.*, *36*, 55–65.

Della Vedova, B., G. Pellis, J. P. Foucher, and J. P. Rehault (1984), Geothermal structure of the Tyrrhenian Sea, *Mar. Geol.*, *55*, 271–289, doi:10.1016/0025-3227(84)90072-0.

Doglioni, C. (1991), A proposal for the kinematic modelling of the Tyrrhenian-Apennines system, *Terra Nova*, *3*, 423–432.

Doglioni, C., E. Gueguen, P. Harabaglia, and F. Mongelli (1999), On the origin of W-directed subduction zones and applications to the western Mediterranean, *Geol. Soc. Spec. Publ.*, *156*, 541–561.

Doglioni, C., F. Innocenti, C. Morellato, D. Procaccianti, and D. Scrocca (2004), On the Tyrrhenian Sea opening, *Mem. Descr. Cart. Geol. d'It.*, *44*, 147–164.

Doglioni, C., E. Carminati, M. Cuffaro, and D. Scrocca (2007), Subduction kinematics and dynamic constraints, *Earth Sci. Rev.*, *83*, 125–175, doi:10.1016/j.earscirev.2007.04.001.

Doglioni, C., et al. (2012), The tectonic puzzle of the Messina area (Southern Italy): Insights from new seismic reflection data, *Sci. Rep.*, *2*, 970, doi:10.1038/srep00970.

Dore', A. G., E. R. Lundin, C. Fichler, and O. Olesen (1997), Patterns of basement structure and reactivation along the NE Atlantic margin, *J. Geol. Soc. London*, *154*, 85–92.

Faccena, C., T. W. Becker, F. P. Lucente, L. Jolivet, and F. Rossetti (2001), History of subduction and back-arc extension in the Central Mediterranean, *Geophys. J. Int.*, *145*, 809–820.

Faccenna, C., M. Mattei, R. Funiciello, and L. Jolivet (1997), Styles of back-arc extension inthe Central Mediterranean, *Terra Nova*, *9*, 126–130.

Favali, P., L. Beranzoli, and A. Maramai (2004), Review of the Tyrrhenian Sea seismicity: How much is still to be known?, *Mem. Descr. Carta Geol. d'It*, *44*, 57–70.

Franke D., D. Savva, M. Pubellier, S. Steuer, B. Mouly, J. L. Auxietre, F. Meresse, and N. Chamot-Rookeb (2014), The final rifting evolution in the South China Sea, *Mar. Petrol. Geol.*, *58*(B), 704–720, doi.10.1016/j.marpetgeo.2013.11.020

Gamberi, F., and M. P. Marani (2004), Deep-sea depositional systems of the Tyrrhenian basin, *Mem. Descr. Carta Geol. d'It.*, *44*, 127–146.

Gibbs, A. D. (1984), Structural evolution of extensional basin margins, *J. Geol. Soc. London*, *141*, 609–620.

Greve, S., H. Paulssen, S. Goes, and M. van Bergen (2014), Shear-velocity structure of the Tyrrhenian Sea: Tectonics, volcanism and mantle (de) hydration of a back-arc basin, *Earth Planet. Sci. Lett.*, *400*, 45–53.

Gueguen, E., C. Doglioni, and M. Fernandez (1997), Lithospheric boudinage in the Western Mediterranean back-arc basins, *Terra Nova*, *9*(4), 184–187.

Ippolito, F., F. Ortolani, and M. Russo (1973), Struttura marginale tirrenica dell'Appennino campano: reinterpretazione di dati di antiche ricerche di idrocarburi, *Mem. Soc. Geol. Ital.*, *12*, 123–132.
Jolivet, L., et al. (1998), Midcrustal shear zones in postorogenic extension: Example from the northern Tyrrhenian Sea, *J. Geophys. Res.*, *103*, 12,123–12,160, doi:10.1029/97JB03616.
Jolivet, L., R. Augier, C. Faccenna, and A. Crespo-Blanc (2008), Subduction, convergence, and the mode of back-arc extension in the Mediterranean region, *Bull. Soc. Géol. France*, *179*(6), 525–550.
Jolivet, L., C. Gorini, J. Smit, and S. Leroy (2015), Continental breakup and the dynamics of rifting in back-arc basins: The Gulf of Lion margin, *Tectonics*, *34*, 662–679, doi:10.1002/2014TC003570.
Kastens, K. A., et al. (1988), O.D.P. Leg 107 in the Tyrrhenian Sea: insights into passive margin and back-arc basin evolution, *Geol. Soc. Am. Bull.*, *100*, 1140–1156.
Kastens, K., and J. Mascle (1990), The geological evolution of the Tyrrhenian Sea: An introduction to the scientific results of ODP Leg 107, in *Proceedings of the Ocean Drilling Program, Scientific Results*, vol. 107, edited by K. Kastens et al., pp. 3–26.
Lagabrielle, Y. (2009), Mantle exhumation and lithospheric spreading: An historical perspective from investigations in the Oceans and in the Alps-Apennines ophiolites, *Ital. J. Geosci.*, *128*(2), 279–293, doi:10.3301/IJG.2009.128.2.279.
Lavier, L. L., and G. Manatschal (2006), A mechanism to thin the continental lithosphere at magma-poor margins, *Nature*, *440*(16), 324–328, doi:10.1038/nature04608.
Ligi, M., L. Cocchi, G. Bortoluzzi, F. D'Oriano, F. Muccini, F. Caratori Tontini, C. E. J. de Ronde, and C. Carmisciano (2014), Mapping of seafloor hydrothermally altered rocks using geophysical methods: Marsili and Palinuro seamounts, southern Tyrrhenian Sea, *Econ. Geol.*, *109*, 2103–2117.
Loreto, M. F., F. Italiano, D. Deponte, L. Facchin, and F. Zgur (2015), Mantle degassing on a near shore volcano, SE Tyrrhenian Sea, *Terra Nova*, *27*(3), 195–205, doi:10.1111/ter.12148.
Lustrino, M., S. Duggen, and C. L. Rosenberg (2011), The Central-Western Mediterranean: Anomalous igneous activity in an anomalous collisional tectonic setting, *Earth Sci. Rev.*, *104*, 1–40.
Malinverno, A. (1981), Quantitative estimates of age and Messinian paleo bathymetry of the Tyrrhenian Sea after seismic reflection, heat flow and geophysical models, *Boll. Geof. Teor. Appl.*, *23*, 159–171.
Malinverno, A., and W. B. F. Ryan (1986), Extension in the Tyrrhenian Sea and shortening in the Apennines as result of arc migration driven by sinking of the lithosphere, *Tectonics*, *5*, 227–245, doi:10.1029/TC005i002p00227.
Marani, M. P., and Trua, T. (2002), Thermal constriction and slab tearing at the origin of a superinflated spreading ridge: Marsili volcano (Tyrrhenian Sea), *J. Geophys. Res.*, *107*(B9), 2188, doi:10.1029/2001JB000285.
Marcuson, R., D. K. Blackman, and N. Harmon (2014), Seismic anisotropy predicted for 2-D plate-driven flow in the Lau back–arc basin, *Phys. Earth Planet. Inter.*, *233*, 88–94.
Mariani, M., and R. Prato (1988), I bacini neogenici costieri del margine tirrenico: Approccio sismicostratigrafico, *Mem. Soc. Geol. Ital.*, *41*, 519–531.
Martinez, F., K. Okino, Y. Ohara, A. L. Reysenbach, and S. K. Goffredi (2007), Back-arc basins, *Oceanography*, *20*(1), 116–127, doi:10.5670/oceanog.2007.85.
Mascle, J., and J. P. Rehault (1990), A revised seismic stratigraphy of the Tyrrhenian Sea: Implications for the basin evolution, in, in *Proceedings of the Ocean Drilling Programme*, *Scientific Results*, vol. 107, edited by K. A. Kastens et al., pp. 617–636 .
McClay, K., and S. Khalil (1998), Extensional hardlinkages, eastern Gulf of Suez, Egypt, *Geology*, *26*, 563–566.
Metrich, N., R. Santacroce, and C. Savelli (1988), Ventotene, a potassic quaternary volcano in central Tyrrhenian Sea, *Rend. Soc. Ital. Mineral. Petrol.*, *43*, 1195–1213.
Milia, A., and M. M. Torrente (2007), The influence of paleogeographic setting and crustal subsidence on the architecture of ignimbrites in the Bay of Naples (Italy), *Earth Planet Sci. Lett.*, *263*, 192–206.
Milia, A., and M. M. Torrente (2015), Tectono-stratigraphic signature of a rapid multistage subsiding rift basin in the Tyrrhenian-Apennine hinge zone (Italy): A possible interaction of upper plate with subducting slab, *J. Geodyn.*, *86*, 42–60.
Milia, A., M. M. Torrente, B. Massa, and P. Iannace (2013), Progressive changes in rifting directions in the Campania margin (Italy): New constrains for the Tyrrhenian Sea opening, *Global Planet. Change*, *109*, 3–17.
Milia, A., P. Iannace, M. Tesauro, and M. M. Torrente (2016a), Upper plate deformation as marker for the Northern STEP fault of the Ionian slab (Tyrrhenian Sea, central Mediterranean), *Tectonophysics*, doi:10.1016/j.tecto.2016.08.017.
Milia, A., A. Valente, G. Cavuoto, and M. M. Torrente (2016b), Miocene progressive forearc extension in the Central Mediterranean, *Tectonophysics*, doi:10.1016/j.tecto.2016.10.002.
Moussat, E., J. P. Rehault, and A. Fabbri (1986), Rifting et evolution tectono-sédimentaire du Bassintyrrhenien au cours du Néogène et du Quaternaire, *Giorn. Geol.*, *48*(1/2), 41–62.
Moy, D. J., and J. Imber (2009), A critical analysis of the structure and tectonic significance of rift-oblique lineaments ('transfer zones') in the Mesozoic–Cenozoic succession of the Faeroe–Shetland Basin, NE Atlantic margin, *J. Geol. Soc. London*, *166*, 831–844, doi:10.1144/0016-76492009-010.
Musacchio, M., G. Carrarra, F. Gamberi, and M. Marani (1999), Tectonic setting of the eastern Tyrrhenian margin, in *Geoitalia* 2° Forum FIST, Bellaria, *SIMP* Riassunti, vol. 1, pp. 184–185.
Parotto, M., and A. Praturlon (1975), Geological summary of Central Apennines, in *Quaderni de "La Ricerca Scientifica"*, vol. 90, pp. 257–311, CNR, Roma.
Pascucci, V., S. Merlini, and I. P. Martini (1999), Seismic stratigraphy of the Miocene–Pleistocene sedimentary basins of the northern Tyrrhenian sea and western Tuscany (Italy), *Basin Res.*, *11*(4), 337–356, doi:10.1046/j.1365-2117.1999.00104.x.
Pascucci, V., A. Costantini, I. P. Martini, and R. Dringoli (2006), Tectono-sedimentary analysis of a complex, extensional, Neogene basin formed on thrust-faulted, Northern Apennines hinterland: Radicofani Basin, Italy, *Sediment. Geol.*, *183*(1–2), 71–97, doi:10.1016/j.sedgeo.2005.09.009.
Patacca, E., R. Sartori, and P. Scandone (1990), Tyrrhenian basin and Apenninic arcs: Kinematic relations since late Tortonian times, *Mem. Soc. Geol. Ital.*, *45*, 425–451.
Peccerillo, A. (2005), Plio-Quaternary volcanism in Italy, in *Petrology, Geochemistry, Geodynamics*, 1–365, Springer, Heidelberg.
Pérez-Gussinyé, M., C. R. Ranero, T. J. Reston, and D. Sawyer (2003), Mechanisms of extension at non volcanic margins: Evidence from the Galicia interior basin, west of Iberia, *J. Geophys. Res.*, *108*(B5), 2245, doi:10.1029/2001JB000901.
Prada, M., V. Sallares, C. R. Ranero, M. G. Vendrell, I. Grevemeyer, N. Zitellini, and R. de Franco (2014), Seismic structure of the Central Tyrrhenian basin: Geophysical constraints on the nature of the main crustal domains, *J. Geophys. Res. Solid Earth*, *119*, 52–70, doi:10.1002/2013JB010527.

Prada, M., V. Sallares, C. R. Ranero, M. G. Vendrell, I. Grevemeyer, N. Zitellini, and R. de Franco (2015), The complex 3-D transition from continental crust to backarc magmatism and exhumed mantle in the Central Tyrrhenian basin, *Geophys. J. Int.*, *203*, 63–78, doi:10.1093/gji/ggv271.

Prada, M., C. R. Ranero, V. Sallares, N. Zitellini, and I. Grevemeyer (2016), Mantle exhumation and sequence of magmatic events in the Magnaghi–Vavilov Basin (Central Tyrrhenian, Italy): New constraints from geological and geophysical observations, *Tectonophysics*, *689*, 133–142, doi:10.1016/j.tecto.2016.01.041.

Ranero, C. R., and M. Pérez-Gussinye (2010), Sequential faulting explains the asymmetry and extension discrepancy of conjugate margins, *Nature*, *468*, 294–300, doi:10.1038/nature09520.

Robin, C., P. Colantoni, M. Genessaux, and J. P. Rehault (1987), Vavilov seamount: A midly alkaline Quaternary volcano in the Tyrrhenian basin, *Mar. Geol.*, *78*, 125–136.

Rossetti, F., F. Balsamo, I. M. Villa, M. Bouybaouenne, C. Faccenna, and R. Funiciello (2008), Pliocene–Pleistocene HT–LP metamorphism during multiple granitic intrusions in the southern branch of the Larderello geothermal field (southern Tuscany, Italy), *J. Geol. Soc. London*, *165*, 247–262, doi:10.1144/0016-76492006-132.

Sandwell, D. T., and W. H. F. Smith (1997), Marine Gravity anomaly from GEOSAT and ERS-1 satellite altimetry, *J. Geophys. Res.*, *102*, 10,039–10,054, doi:10.1029/96JB03223.

Sartori, R., L. Torelli, N. Zitellini, G. Carrara, M. Matteo, and P. Mussoni (2004), Crustal features along a W–E Tyrrhenian transect from Sardinia to Campania margins (Central Mediterranean), *Tectonophysics*, *383*(3–4), 171–192, doi:10.1016/j.tecto.2004.02.008.

Savelli, C. (1984), Eta' K/Ar delle principali manifestazioni riolitiche dell'isola di Ponza, *Rend. Soc. Geol. Ital.*, *6*, 39–42.

Savelli, C. (1987), K/Ar ages and chemical data of volcanism in the western Pontine Islands (Tyrrhenian Sea), *Boll. Soc. Ital.*, *106*, 356–546.

Savelli, C. (1988), Late Oligocene to recent episodes of magmatism in and around the Tyrrhenian Sea: Implications for the processes of opening in a young inter-arc basin of intra-orogenic (Mediterranean) type, *Tectonophysics*, *146*, 163–181.

Schellart, W. P., G. S. Lister, and M. W. Jessell (2002), Analogue modeling of arc and backarc deformation in the New Hebrides arc and North Fiji Basin, *Geology*, *30*, 311–314.

Schellart, W. P., M. W. Jessell, and G. S. Lister (2003), Asymmetric deformation in the backarc region of the Kuril arc, northwest Pacific: new insights from analogue modeling, *Tectonics*, *22*(5), 1047, doi:10.1029/2002TC001473.

Schettino, A., and E. Turco (2011), Tectonic history of the western Tethys since the Late Triassic, *Geol. Soc. Am. Bull.*, *123*(1–2), 89–105.

Scrocca, D., C. Doglioni, F. Innocenti, P. Manetti, A. Mazzotti, L. Bertelli, S. Burbi, and D. D'Offizi (2003a), CROP atlas: Seismic reflection profiles of the Italian crust, *Mem. Descr. Carta Geol. Ital.*, *62*, 1–194.

Scrocca, D., C. Doglioni, and F. Innocenti (2003b), Constraints for an interpretation of the Italian geodynamics: A review, in *CROP Atlas: Seismic Reflection Profiles of the Italian Crust*, *Mem. Descr. Carta Geol. It*, vol. 62, edited by D. Scrocca, pp. 15–46.

Scrocca, D., E. Carminati, C. Doglioni, and D. Procaccianti (2012), Tyrrhenian Sea, in *Regional Geology and Tectonics: Phanerozoic Passive Margins, Cratonic Basins and Global Tectonic Maps*, vol. 1C, edited by D. G. Roberts and A. W. Bally, pp. 473–485, Elsevier, Amsterdam.

Spadini, G., and F. C. Wezel (1994), Structural evolution of the "41st parallel zone": Tyrrhenian Sea, *Terra Nova*, *6*, 552–562.

Tsikalas, F., J. I. Faleide, and O. Eldholm (2001), Lateral variations in tectono-magmatic style along the Lofoten-Vesteralen volcanic margin off Norway, *Mar. Pet. Geol.*, *18*, 807–832.

Turco, E., A. Schettino, P. P. Pierantoni, and G. Santarelli (2010), The Pleistocene extension of the Campania Plain in the framework of the Southern Tyrrhenian tectonic evolution: morphotectonic analysis, kinematic model and implications for volcanism, in *Volcanism in the Campania Plain–Vesuvius, Campi Flegrei and Ignimbrites*, *Dev. Volcano.*, vol. 9, edited by B. De Vivo, pp. 27–51.

Vignaroli, G., G. Berardi, A. Billi, S. Kele, F. Rossetti, M. Soligo, and S. M. Bernasconi (2016), Tectonics, hydrothermalism, and paleoclimate recorded by Quaternary travertines and their spatio-temporal distribution in the Albegna basin, central Italy: Insights on Tyrrhenian margin neotectonics, *Lithosphere*, *8*(3), doi:10.1130/L507.1.

Whitmarsh, R. B., and P. Wallace (2001), The rift-to-drift development of the west Iberia nonvolcanic continental margin: A summary and review of the contribution of ocean drilling program leg 173, *Proc. Ocean Drill. Project Sci. Results*, *173*, 1–36.

Yilmaz, O. (2001), Seismic data analysis: Processing, inversion and interpretation of seismic data, *Society of Exploration Geophysicists*, 1–2065, doi:10.1190/1.9781560801580.

Zitellini, L., M. Marani, and A. M. Borsetti (1984), Post-orogenic tectonic evolution of Palmarola and Ventotene basins (Pontine archipelago), *Mem. Soc. Geol. It.*, *27*, 121–131.

Zito, G., F. Mongelli, S. De Lorenzo, and C. Doglioni (2003), Heat flow and geodynamics in the Tyrrhenian Sea, *Terra Nova*, *15*(6), 425–432.